Report No. 173 / UILU ENG-96-4001

The Variables Influencing the Fatigue Behavior of Structural Weldments

by

F. V. Lawrence
S. D. Dimitrakis
W. H. Munse

Submitted to the ASM for inclusion in a Handbook

January 1996

Table of Contents

List of Symbols

a, a_i	Crack length , initial crack length
a_p	Peterson's constant
A	Axial loading
AB	Deep section loaded under bending but stress at hot-spot pseudo-axial
b	Cyclic strength exponent
B	Effects of fabrication distortion
B	Bending stresses
c	Cyclic ductility exponent
C	Crack initiation site due to tensile stresses
C_s	Crack initiation site due to shear stresses
C, C'	Coefficient in Paris Power Law, same for effective stress intensity
COV	Coefficient of variation
da/dN	Fatigue crack growth rate
E	Young's modulus
F	Flame cut edges
G	Weld ground
G	Effects of notch severity
GMAW	Gas-metal-arc welding process
GTAW	Gas-tungsten-arc welding process
HAZ	Heat affected zone
IJP	Incomplete joint penetration
K	Monotonic strength coefficient
K'	Cyclic strength coefficient
K_f	Fatigue notch factor
K_{feff}	Maximum effective fatigue notch factor
K_{IC}	Fracture toughness
K_t	Stress concentration factor at notch root
L	Length of intermittent weld
M	Machined surfaces
m, m_p	Paris exponent
M_k	Weld geometry correction factor
MS	Effects of applied mean stress
n	Monotonic strength exponent
n'	Cyclic strength exponent
N_I	Crack initiation life
N_N	Crack nucleation life
N_{P1}	Short crack propagation life
N_{P2}	Long crack propagation life
N_T	Total fatigue life
P	Pitch between two intermittent welds
R	Stress ratio
r	Notch root radius, also correlation coefficient
R_F	Fatigue life reduction factor to assure a certain reliability
RS	Effects of residual stress
RSW	Resistance spot welding
s	Standard deviation
S_a	Applied stress amplitude
S_{fab}	Fabrication stresses
SMAW	Shielded-metal-arc welding process
S_u	Ultimate strength

S_y	Yield strength
S_{yBM}	Base metal yield strength
$S_{50\%}$	Applied stess range associated with a 50 % probability of no failure
$S_{95\%}$	Applied stess range associated with a 95 % probability of no failure
T	Plate thickness
W	Plate width
WM	Weld metal
x	Degree of bending
Y	Geometry correction factor for fatigue crack growth
ΔK	Stress intensity factor range
ΔP	Applied load range
ΔS	Applied stress range
ΔS_a	Axial applied stress range
ΔS_b	Bending applied stress range
ΔS_{design}	Design stress range
$\Delta S_{smooth\ specimen}$	Mean fatigue strength of a smooth specimen
$\Delta S_{plain\ plate}$	Mean fatigue strength of a plain plate
ΔS_{max}	Maximum applied stress range
ΔS_{mean}	Mean fatigue strength
ΔS_{weld}	Mean fatigue strength of a weld
$\Delta S_{weldment}$	Mean fatigue strength of a weldment
ε'_f	Cyclic ductility coefficient
θ	Weld flank angle
σ_r	Welding residual stresses at the notch root
σ'_f	Cyclic strength coefficient
Ω_S	COV of the fatigue strength of a weldment.
Ω_P	COV of the random variable for the effects of material properties.
Ω_G	COV of the random variable for the stress-concentrating effects of geometry.
Ω_B	COV of the random variable for the effects of fabrication residual stresses.
Ω_{RS}	COV of the random variable for the effects of notch-root residual stress.
Ω_{MS}	COV of the random variable for the effects of applied mean stress.

1. Major Variables Affecting the Fatigue Life of Weldments

While there are many variables which affect the fatigue life of weldments, it could be said that the fatigue resistance of a weldment is really controlled by :

- The presence or absence of weld discontinuities at the root of the critical notch.
- The size of the weldment.
- The magintude of the residual stresses which develop during fabrication.

In this article, we will compare and contrast the behavior of discontinuity-containing ("Nominal") weldments and discontinuity-free ("Ideal") weldments fabricated from thin (0.5-in.) or thick (2.0-in.) plates, with or without significant fabrication residual stresses.

2. Stages in the Fatigue Life of Weldments

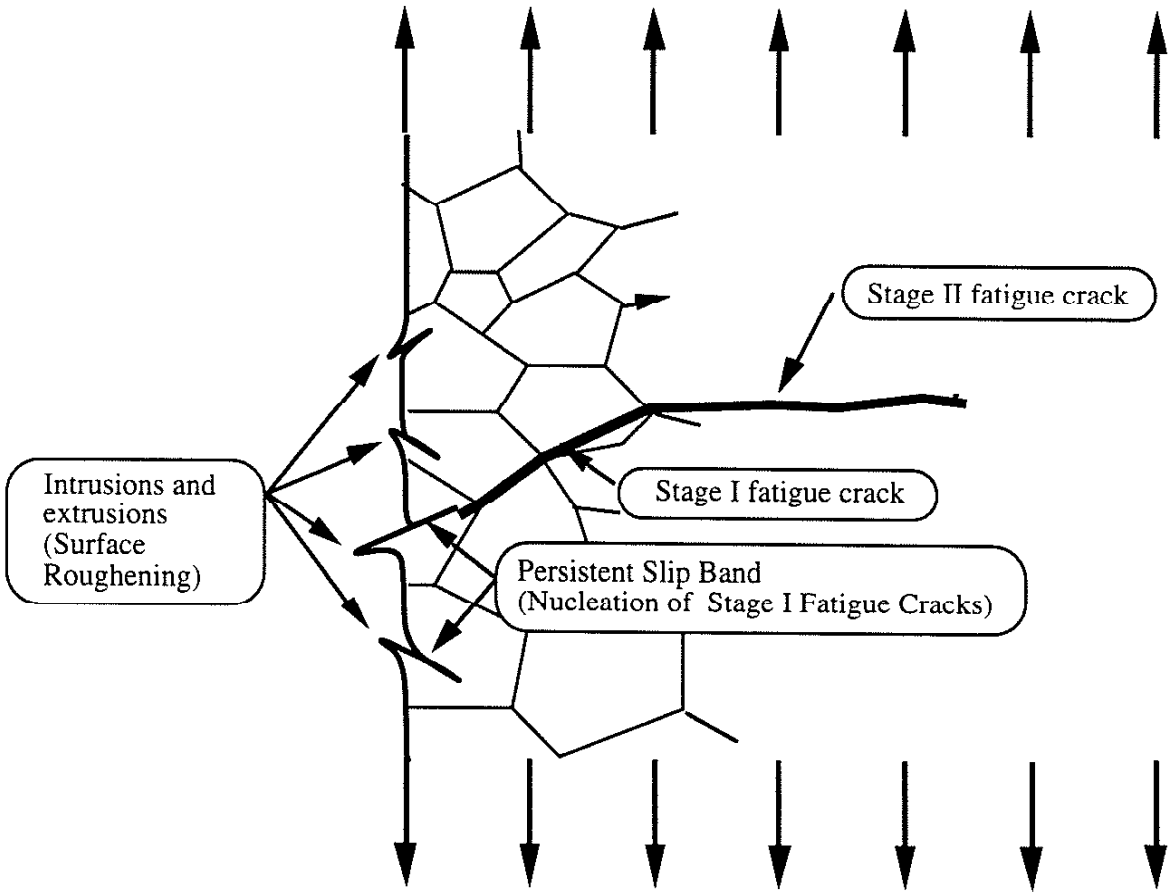

Fig. 1.1 Metallic fatigue: The stages of fatigue include cyclic slip (crack nucleation), Stage I, and Stage II crack growth.

2.1 The Process of Metallic Fatigue in Weldments

As with any notched metal component, the process of fatigue in weldments may be divided into three periods: crack nucleation, the development and growth of a short crack (Stage I), and the growth of a dominant (long) crack to a length at which it either arrests or causes fracture (Stage II): see Fig. 2.1.

The boundaries between these periods are ill-defined. Nonetheless, it is useful to think of the total fatigue life of a notched metal component or a weldment (N_T) as the sum of three life periods: fatigue crack nucleation (N_N), short (or Stage I) crack growth (N_{P1}), and long (or Stage II) crack growth (N_{P2}).

$$N_T = N_N + N_{P1} + N_{P2} \tag{2.1}$$

The relative contribution of each of these three periods to the fatigue life of weldments is controversial and appears to vary with the geometry of the weld and weldment, the size of the weldment, the nature of the residual stresses present, and the severity of the weld discontinuities existing in the weldment. In this article, it will be useful to imagine that there are two extreme kinds of weldments: "Nominal" weldments which contain substantial (≈0.1 in. depth) weld discontinuities and "Ideal" weldments which have blended weld toes and no substantial weld discontinuities. As will be seen, the fatigue behavior of the "Nominal" and "Ideal" weldments differs greatly.

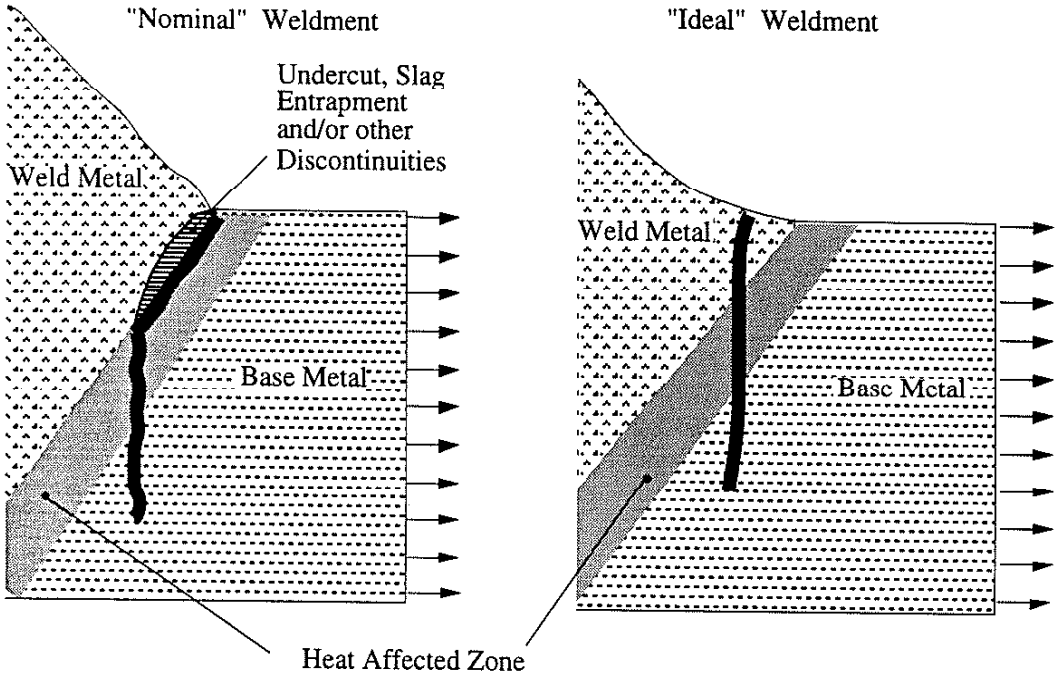

Fig. 2.2 Conceptual drawing of fatigue crack initiation and growth at the toe of (left) a "Nominal" weldment having a substantial (≈0.1 in. depth) weld discontinuity (slag entrapment) at the root of the critical notch (weld toe) and (right) an "Ideal" weldment with good wetting and no substantial discontinuity at the root of the critical notch.

2.2 Conditions Leading to the Dominance of Long Crack Growth (N_{P2})

For many reasons, Stage II crack growth generally dominates the fatigue life of a weldment, while the periods devoted to crack nucleation (N_N) and early crack growth (N_{P2}) are generally relatively short. Engineers for whom a single failure would be catastrophic and who are

forced to use low-quality welding procedures must by necessity adopt a very pessimistic view regarding the fatigue life of weldments and make the rather conservative assumption:

$$N_T \approx N_{P2} \tag{2.2}$$

The basic geometry and/or loading of some weldments leads to a very desirable phenomenon in which a Stage II crack slows down rather than accelerates as the crack lengthens. Whenever this occurs, the growth[1] of long cracks (N_{P2}) can be a major fraction of their fatigue life and such weldments may never fail but develop long, slow-growing fatigue cracks: see Fig. 2.3.

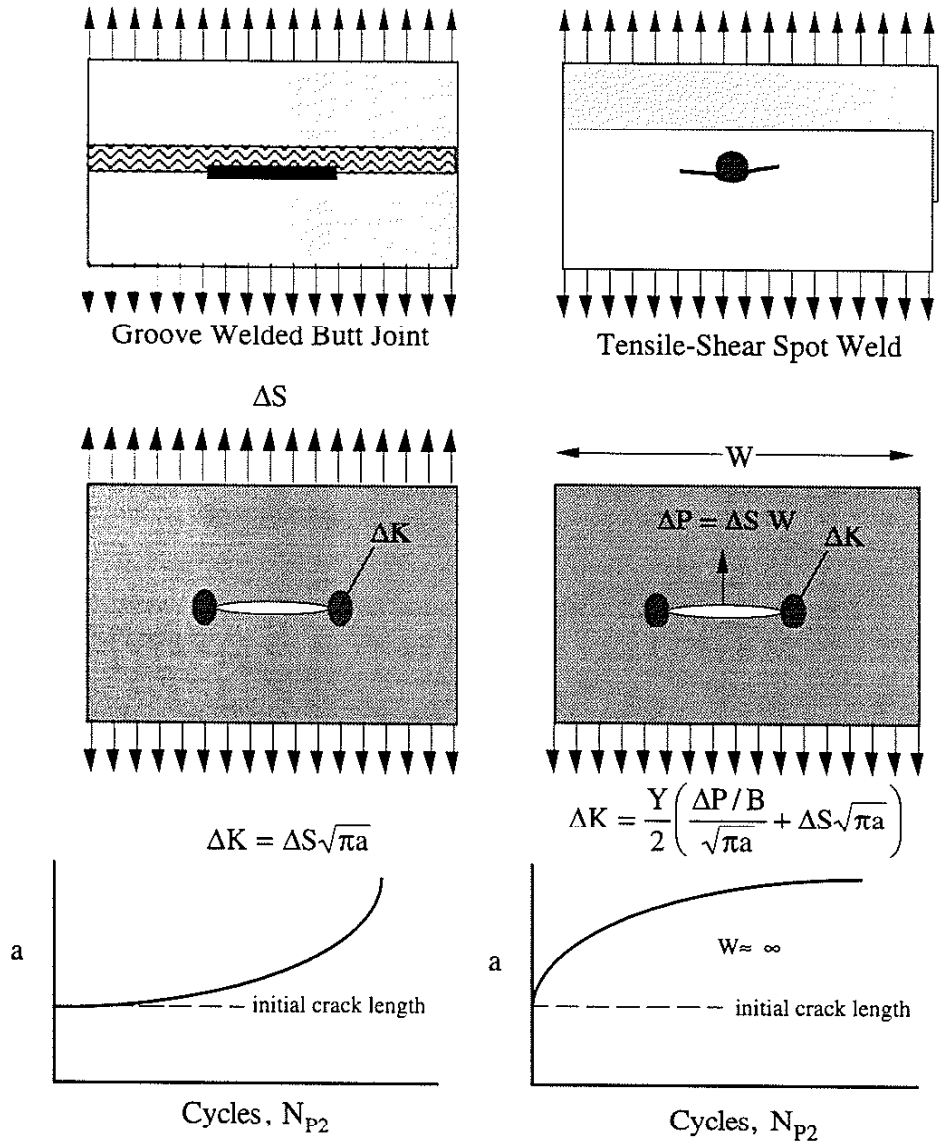

Fig. 2.3 Two radically dissimilar patterns of Stage II crack growth in weldments[2]. Most weldments have several sites of stress concentration.

[1] Recall that the growth rate of fatigue cracks (da/dN) is controlled by the range of stress intensity factor (ΔK): da/dN = $C(\Delta K)^n$ (the Paris Power Law).

[2] All symbols have their conventional meaning: see List of Symbols.

Corrosion fatigue is a third phenomenon which diminishes the relative importance of crack nucleation (N_N) and small crack growth (N_{P1}) in weldments. Finally, variable load histories containing many large, damaging events may greatly shorten the fatigue life devoted to N_N and N_{P1}.

2.3 Conditions Favoring Crack Nucleation and Early Crack Growth

While the deleterious effects of weld discontinuities, corrosion fatigue, and some variable load histories can diminish the importance of N_N and N_{P1} in weldments, one can also adopt an opposite, more optimistic view of the fatigue life of weldments in which N_N and N_{P1} can be a major part of the fatigue life of a weldment and in which the fatigue life of such an "Ideal" weldment can be greater than N_{P2}. "Fluxless" fusion welding processes such as gas-metal-arc welding (GMAW) or gas-tungsten-arc welding (GTAW) are capable of producing large weldments in which 0.1 in. weld discontinuities at the root of the critical notch are few or even non-existent[3]. Even ordinary welding processes such as resistance spot welding (RSW) produce weldments in which large discontinuities are not found. Thus, high quality structural welds and other welds such as resistance spot welds may not contain large discontinuities, and their behavior may approach that of an "Ideal" weldment. In some applications, only a few welded locations are highly stressed and thus critical. In such a circumstance, the probability of a serious discontinuity being present in the critical location is sufficiently remote that the majority of the population of the welded components can be considered discontinuity free and will behave like the "Ideal" weldment. Many situations involve constant amplitude or pseudo-constant-amplitude loading, and thus the concern about variable load histories may be lessened. Finally, there are welding procedures and post-weld treatments which can substantially improve the fatigue life of a weldment through increases in any or all of the life periods N_N, N_{P1} and N_{P2}.

This optimistic view is certainly a goal for manufacturers who must produce high-quality but low-cost or low-weight components. In this circumstance, it is reasonable to think of the fatigue life of a weldment as approaching that of the "Ideal' weldment, as depending upon N_N and N_{P1}, and as unlike the "Nominal" weldment susceptible to large improvement.

2.4 Scope of the Article

The fatigue strength of weldments is a factor of 1.5 to 5 less than that of plain plate. In this article, we will adopt the view that there are two basic types of weldments: "Nominal" weldments in which N_{P2} dominates and "Ideal" weldments in which N_N and N_{P1} are much more important.

In the next chapter, we will examine the role of joint geometry and systems for their classification in determining the allowable design stresses. The variety of weldment geometries is a major fatigue variable; unfortunately there are an essentially infinite number of joint configurations, and it is impossible to make an exhaustive catalogue. Moreover, despite the wealth of experimental information, only limited conclusions can be drawn regarding many of the variables influencing the fatigue behavior of weldments because of the scatter in the experimental data.

Therefore, in the last chapter we will use a computer simulation model to explore the influence of the important variables which influence the mean fatigue strength of an individual structural steel weldment.

---

[3] It should be noted that for a weld discontinuity to control the fatigue resistance of a weldment, it must be located at the root of the critical notch so that the worst case can occur in which the stress concentrations of both the critical notch and the weld discontinuity interact. The fact that fatigue invariably begins at the root of the critical notch reduces the likelihood of randomly distributed weld discontinuities participating in fatigue crack nucleation and early crack growth which are constrained to the root of the critical notch, that is, the ripple, the toe, or the root of a weldment. It is also possible that the weld reinforcement may be sufficiently irregular so that the worst notch can be located in the weld metal; however, this situation can be avoided by proper welding.

3. The Effects of Weldment Joint Geometry

3.1 The Fatigue Behavior of 53 Structural Details

Some of the common structural details encountered in bridge construction, ship, and ground-vehicle construction have been catalogued[4] by Munse et al. [1]. The shapes of 53 structural details and variations of these details are shown in Fig. 3.1 The abbreviations used are given in Table 3.1 and further information regarding the 53 joints is given in Table 3.2. This catalogue begins with what would seem to be the simplest shapes and proceeds toward the more complex. Some of the final geometries (e.g. #39) are complex weldments and should really be considered to be structures. Note that the classification system includes bolted and riveted joints (#8 and #9) and plug and spot welds (#27) which as argued in the previous section behave in a fundamentally different way. Several details (# 28 and #29) are not connections but simply notched components. For this reason, we shall at first refer to the items in the catalogue as structural details; but later, we will focus our attention on the welded details.

TABLE 3.1 ABBREVIATIONS USED IN THE TABLES OF CHAPTER 3

(F)	-	flame cut edges
(G)	-	weld ground
(B)	-	bending stresses
(M)	-	machined surfaces
(P)	-	principal stresses
(S)	-	shear stresses
A, B, C, ...	-	additional description within the same detail number
C→	-	crack initiation site due to tensile stresses
C_S→	-	crack initiation site due to shear stresses
L	-	length of intermittent weld
P	-	pitch between two intermittent welds
R	-	radius
t	-	thickness of plate

[4] Munse's numbering system is related to that of the AISC [3] but the AISC classification of weldments contained only 27 shapes.

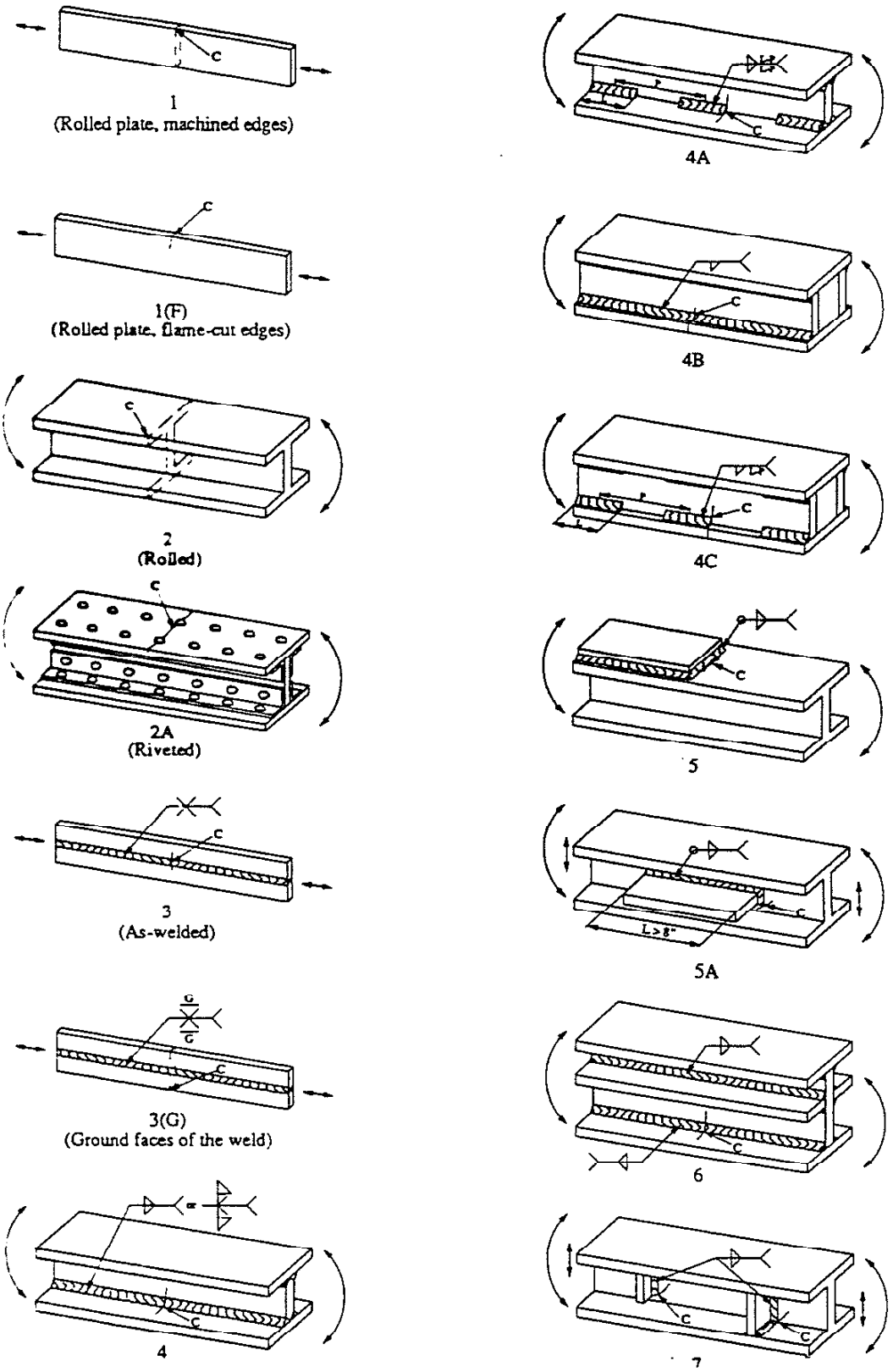

Fig. 3.1 Fifty-three structural details commonly encountered in bridge, ship, and ground-vehicle construction [1].

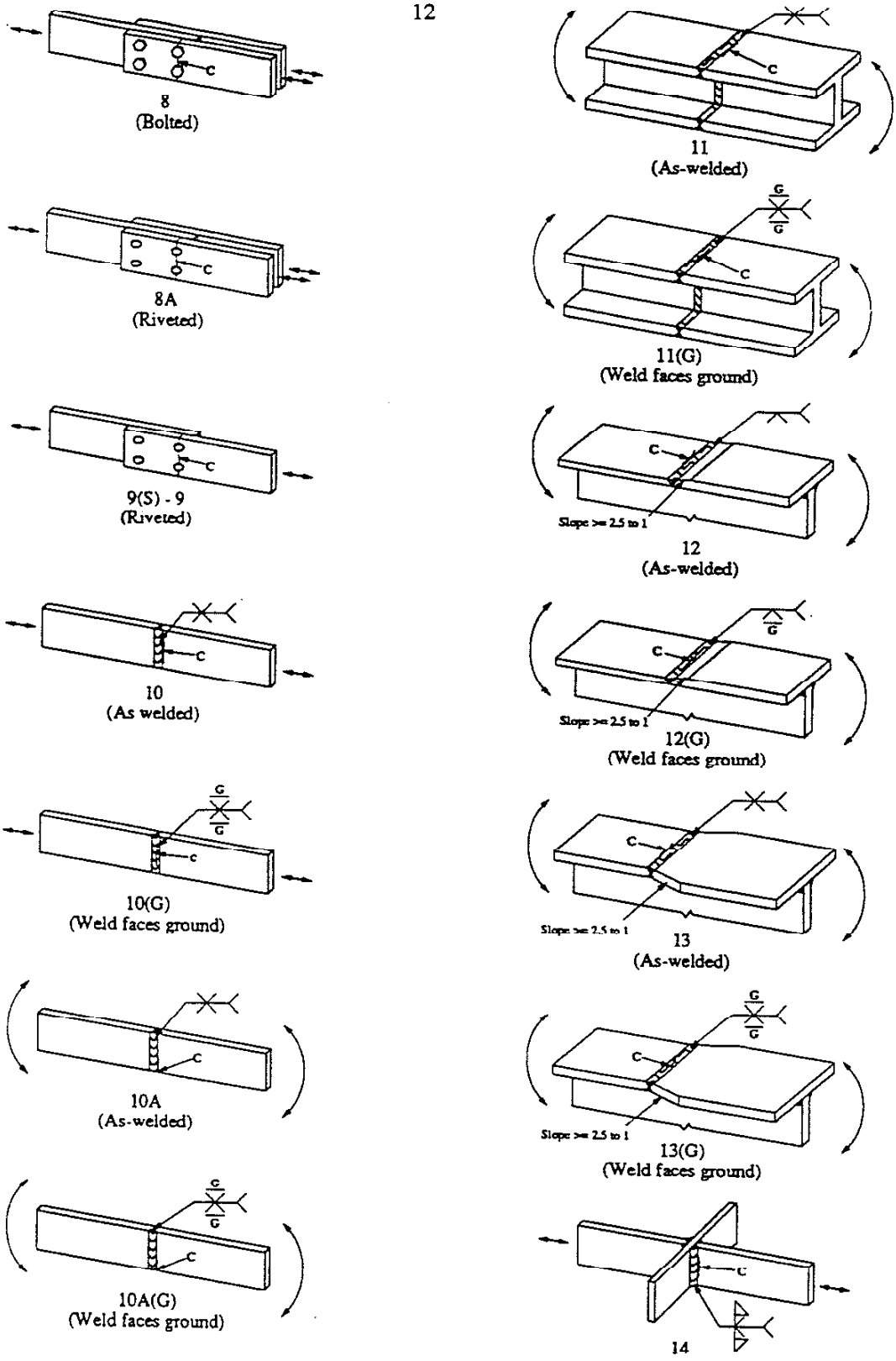

Fig. 3.1 Fifty-three structural details commonly encountered in bridge, ship, and ground-vehicle construction [1].

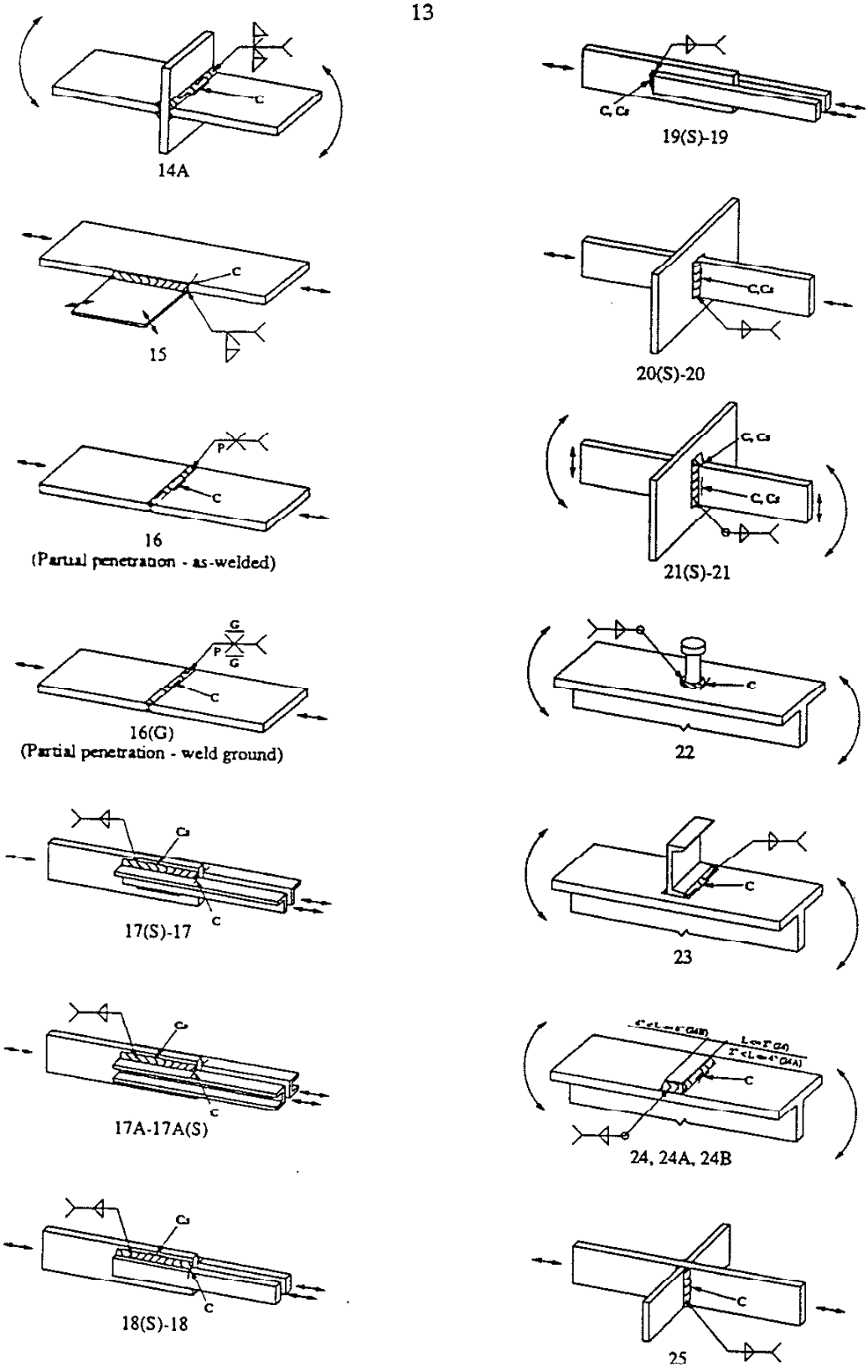

Fig. 3.1 Fifty-three structural details commonly encountered in bridge, ship, and ground-vehicle construction [1].

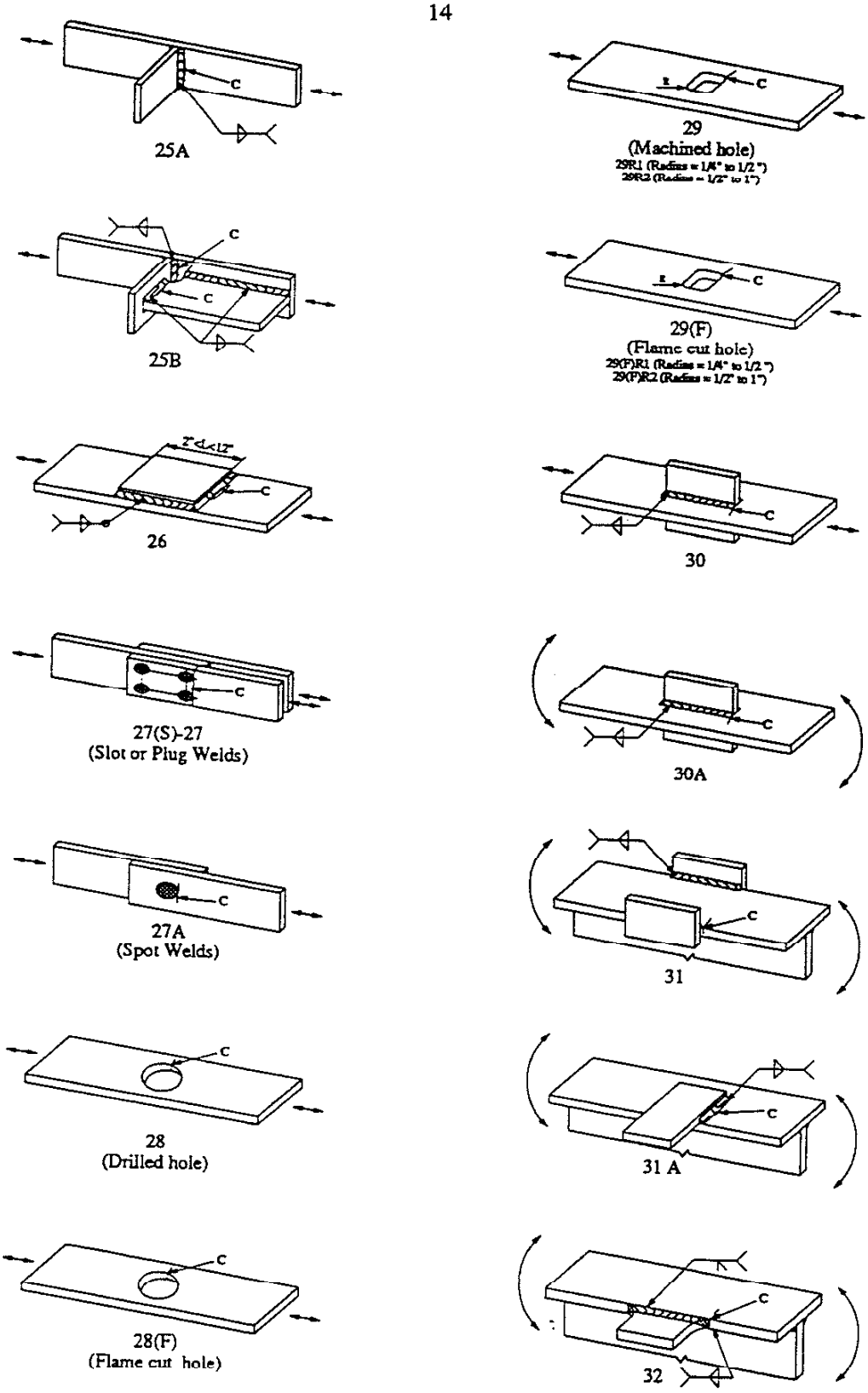

Fig. 3.1 Fifty-three structural details commonly encountered in bridge, ship, and ground-vehicle construction [1].

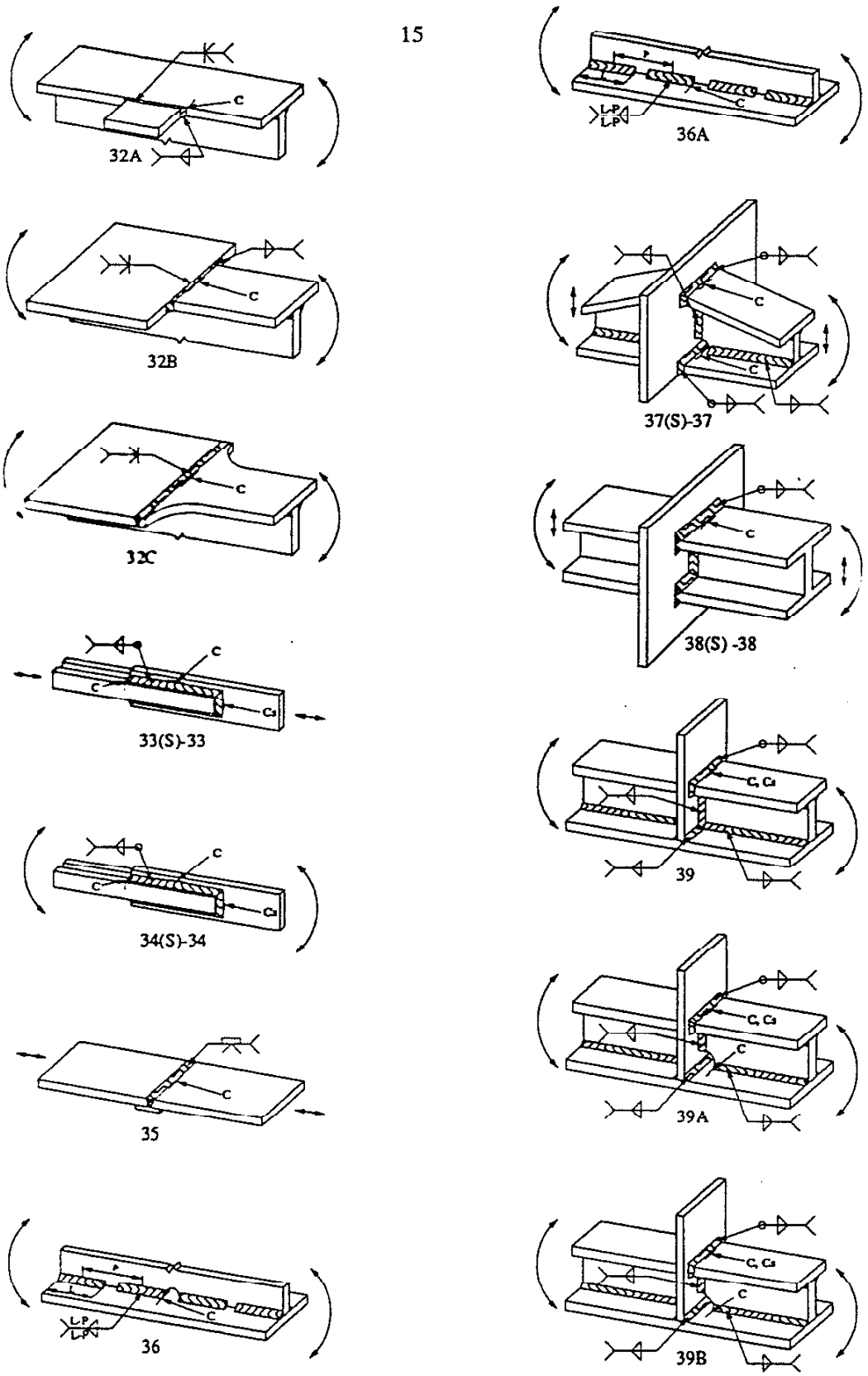

Fig. 3.1 Fifty-three structural details commonly encountered in bridge, ship, and ground-vehicle construction [1].

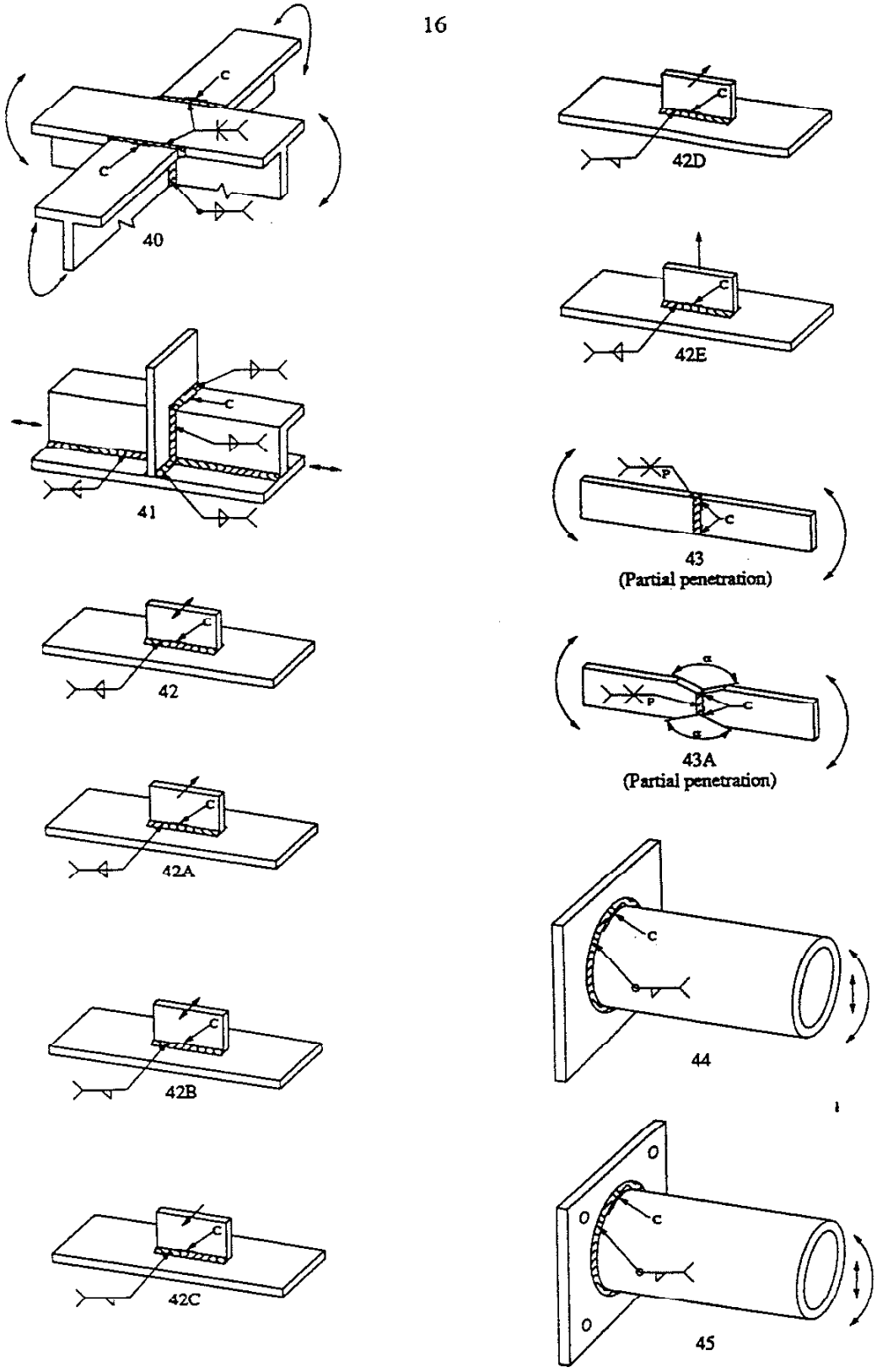

Fig. 3.1 Fifty-three structural details commonly encountered in bridge, ship, and ground-vehicle construction [1].

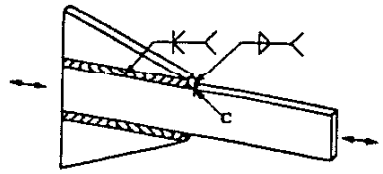

46

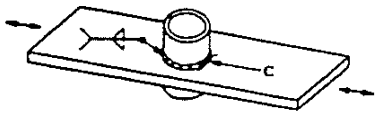

47
(Tube passes through)

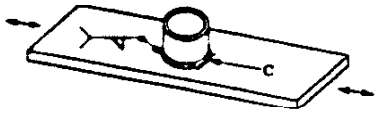

47A

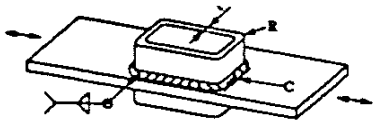

48 (R = 2t)
48R (R > 2t)
(Tube passes through)

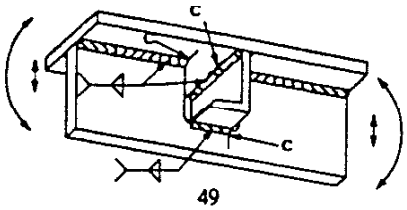

49

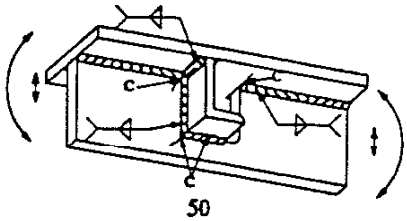

50

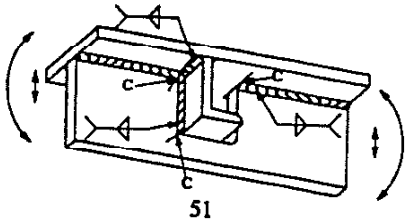

51

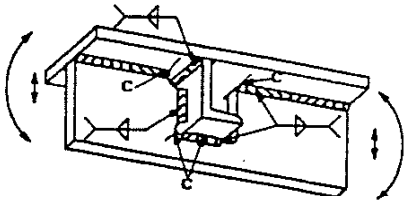

52

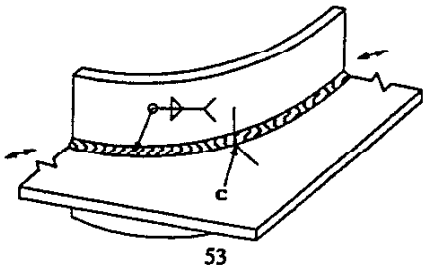

53

Fig. 3.1 Fifty-three structural details commonly encountered in bridge, ship, and ground-vehicle construction [1].

TABLE 3.2 STRUCTURAL DETAIL CATALOGUE [1]

Detail number	Detail description	Loading condition	Fatigue crack initiation site
1	Plain plate, machined edges	Axial	Corners
1(F)	Plain plate, flame-cut edges	Axial	Edges
2	Rolled I-beam	Bending	Corners
2A	Riveted I-beam	Bending	Holes
3	Longitudinally welded plate, as-welded	Axial	Ripple
3(G)	Longitudinally welded plate, weld ground	Axial	Corners or discontinuity
4	Welded I-beam, continuous weld	Bending	Ripple
4A	Welded I-beam, intermittent weld	Bending	End of weld
4B	Welded box, continuous weld	Bending	Ripple
4C	Welded box, intermittent weld	Bending	End of weld
5	I-beam with welded cover plate	Bending	Weld toe
5A	I-beam with welded plate to web	Bending, shear	Weld toe
6	Welded I-beam with longitudinal stiffeners welded to web	Bending	Ripple
7(B)	I-beam with welded stiffeners	Bending	Weld toe
7(P)	I-beam with welded stiffeners	Bending, shear	Weld toe
8	Double shear bolted lap joint	Axial	Holes
8A	Double shear riveted lap joint	Axial	Holes
9	Single shear riveted lap joint	Axial	Holes
10	Transverse butt joint, as-welded	Axial	Weld toe
10(G)	Transverse butt joint, weld ground	Axial	Weld
10A	Transverse butt joint, as-welded	In-plane bending	Weld toe
10A(G)	Transverse butt joint, weld ground	In-plane bending	Weld
11	Transverse butt welded I-beam, as-welded	Bending	Weld toe
11(G)	Transverse butt welded I-beam, weld ground	Bending	Weld
12	Flange splice (unequal thickness), as-welded	Bending	Weld toe
12(G)	Flange splice (unequal thickness), weld ground	Bending	Weld
13	Flange splice (unequal width), as-welded	Bending	Weld toe
13(G)	Flange splice (unequal width), weld ground	Bending	Weld
14	Cruciform joint	Axial	Weld corner
14A	Cruciform joint	Bending	Weld toe
15	Lateral attachment to plate edge	Axial	End of weld
16	Partial penetration butt weld, as-welded	Axial	Weld toe or weld
16(G)	Partial penetration butt weld, weld ground	Axial	Weld metal
17	Angle welded to plate, longitudinal weld only	Axial	End of weld
17(S)	Angle welded to plate, longitudinal weld only	Axial	Weld
17A(S)	Channel welded to plate, longitudinal weld only	Axial	Weld
17A	Channel welded to plate, longitudinal weld only	Axial	End of weld
18	Flat bars welded to plate, longitudinal weld only	Axial	End of weld
18(S)	Flat bars welded to plate, longitudinal weld only	Axial	Weld
19	Flat bars welded to plate, lateral welds only	Axial	Weld
19(S)	Flat bars welded to plate, lateral welds only	Axial	Weld
20	Cruciform joint	Axial	Weld toe
20(S)	Cruciform joint	Axial	Weld
21	Cruciform joint, 1/4" weld,	In-plane bending	Weld toe
	Cruciform joint, 3/8" weld	Shear	Weld toe
21(S)	Cruciform joint, 1/4" weld,	In-plane bending	Weld
	Cruciform joint, 3/8" weld	Shear	Weld toe
22	Attachment of stud to flange	Bending	Weld toe
23	Attachment of channel to flange	Bending	Weld toe

24 (2L < 4")	Attachment of bar to flange	Bending	Weld toe
24A (L ≤ 2")	Attachment of bar to flange	Bending	Weld toe
24B (4"< L < 8")	Attachment of bar to flange	Bending	Weld toe
25	Lateral attachments to plate	Axial	Weld toe
25A	Lateral attachment to plate	Axial	Weld toe
25B	Lateral attachment to plate with stiffener	Axial	Weld toe or end of weld
26	Doubler plate welded to plate	Axial	Weld toe
27	Slot or plug welded double lap joint	Axial	End of weld nugget
27(S)	Slot or plug welded double lap joint	Axial	Weld nugget
27A	Spot welded single lap joint	Axial	End of weld nugget
27A(S)	Spot welded single lap joint	Axial	Weld nugget
28	Plain plate with drilled hole	Axial	Edge of hole
28(F)	Plain plate with flame-cut circular hole	Axial	Edge of hole
29	Plain plate with machined rectangular hole (R<=1/4")	Axial	Corner of hole
29R1	Plain plate with machined rectangular hole (1/4"< R ≤ 1/2")	Axial	Corner of hole
29R2	Plain plate with machined rectangular hole (1/2"< R ≤ 1")	Axial	Corner of hole
29(F)	Plate with flame-cut rectangular hole (R ≤ 1/4")	Axial	Corner of hole
29(F) R1	Plain plate with flame-cut rectangular hole (1/4"< R ≤ 1/2")	Axial	Corner of hole
29(F) R2	Plain plate with flame-cut rectangular hole (1/2"< R ≤ 1")	Axial	Corner of hole
30	Longitudinal attachments to plate	Axial	Plate at end of weld
30A	Longitudinal attachments to plate	Bending	Plate at end of weld
31	Attachments of plate to edge of flange	Bending	Flange at end of weld
31A	Lateral attachment of plate to flange	Bending	Flange at weld toe
32	Groove welded attachment of radiused plate to edge of flange	Bending	Flange at end of weld
32A	Groove welded attachment of plate to edge of flange	Bending	Flange at end of weld
32B	Butt welded flange (unequal width)	Bending	Weld toe
32C	Butt welded flange (unequal width, radiused transition)	Bending	Weld toe
33	Flat bars welded to plate, lateral and longitudinal welds	Axial	End of weld
33(S)	Flat bars welded to plate, lateral and longitudinal welds	Axial	Weld
34	Flat bars welded to plate, lateral and longitudinal welds	In-plane bending	End of weld
34(S)	Flat bars welded to plate, lateral and longitudinal welds	In-plane bending	Weld
35	Butt joint with backing bar	Axial	Weld toe
36	Welded beam with intermittent welds and cope hole in the web	Bending	End of weld or cope hole
36A	Welded beam with staggered intermittent welds	Bending	End of weld
37	Beam connection with sloping flanges	Bending	Weld toe or end of weld at cope hole
37(S)	Beam connection with sloping flanges	Shear	Weld
38	Beam connection with horizontal flanges	Bending	Weld toe
38(S)	Beam connection with horizontal flanges	Shear	Weld
39	Beam bracket without cope hole	Bending	Weld toe
39A	Beam bracket with round cope hole in web	Bending	Weld toe or end of weld at cope hole
39B	Beam bracket with straight cope hole in web	Bending	Weld toe or end of weld at cope hole
40	Interconnecting beams	Bending in perp.directions	Weld toe
41	Beam bracket	Axial	Weld toe

42	Lateral attachment of plate to plate with weld beads on both sides	Lateral (reversal)	Weld toe
42A	Lateral attachment of plate to plate with weld beads on both sides	Lateral one direction	Weld toe
42B	Lateral attachment of plate to plate with weld bead on one side	Lateral (reversal)	Weld root
42C	Lateral attachment of plate to plate with weld bead on one side	Lateral one direction toward the weld	Weld root
42D	Lateral attachment of plate to plate with weld bead on one side	Lateral one direction away from the weld	Weld toe away from the weld
42E	Lateral attachment of plate to plate with weld beads on both sides	Axial in attachment	Weld toe
43	Partial penetration butt weld, as-welded	In-plane bending	Weld corner or weld
43A	Partial penetration butt weld, with edges notched at weld	In-plane bending	Weld corner or weld
44	Tube welded to plate	Bending, shear	Weld toe
45	Tube welded to flange plate	Bending, shear	Weld toe
46	Triangular gusset attachments to plate	Axial	End of weld
47	Penetrating tube welded to plate	Axial in plate	Weld toe
47A	Attachment of tube to plate	Axial in plate	Weld toe
48 (R = 2t)	Penetrating rectangular tube welded to plate	Axial in plate	Weld toe
48R (R > 2t)	Penetrating rectangular tube welded to plate	Axial in plate	Weld toe
49	Clearance cut-out	Bending, shear	Weld toe or end of weld
50	Clearance cut-out	Bending, shear	Weld toe or end of weld
51	Clearance cut-out	Bending, shear	Weld toe or end of weld
52	Clearance cut-out	Bending, shear	Weld toe or end of weld
53	Reinforced deck cut-out	Axial	Weld ripple

3.2 The Influence of Structural Detail Geometry on Fatigue Strength

The mean strength data in Table 3.3 suggests that (after the applied stress range) detail geometry is the most important variable affecting a structural detail's fatigue life. The role of geometry can be better assessed if fatigue-data-bank information is edited to suppress the effects of other variables such as R ratio and material strength[5]. In Table 3.3 below, the fatigue-data-bank information for many of the structural details listed in Table 3.2 was reanalyzed and restricted to data for R = 0 tests and data for steels having yield strength less than 50 ksi. (345 MPa). In several instances, the AISC classification of the joint was altered by this procedure: see Table 3.3.

3.3 Scatter of Structural Detail Fatigue Data Resulting From Classification Systems

The design stresses which an engineer must adopt are as much controlled by the scatter in the fatigue data as by the mean value of strength for a certain design life. Thus, the uncertainty (scatter) in weldment fatigue life is as much or more important than the mean value. This scatter has two basic sources: "real" scatter which results from the random nature of the fatigue variables controlling the fatigue resistance of a detail and the contribution to the "apparent" scatter which is an artifact of the classification system imposed. The simplest classification scheme is suggested by Fig. 3.1 and Table 3.2. Each detail shape is placed in a class by itself. However, as demonstrated in the previous section, grouping together data for tests having different experimental conditions leads to artifically large values in standard deviation of the log of strength (s). Furthermore, as will be argued below, the practice producing the greatest amount of apparent scatter is the use of broad

[5] It is customary to group together fatigue data for all thickness, strengths, and R ratio. This practice is inadvisable and leads to an unnecessarily large scatter in fatigue data information. It is the opinion of the authors that all data banks should be restricted to a standard strength, R ratio, and thickness.

classification systems in which details having only roughly similar fatigue resistances are grouped together.

TABLE 3.3 COMPARISON OF UNEDITED AND STANDARDIZED FATIGUE DATA FOR STRUCTURAL DETAILS

Details	Mean Fatigue Strength ΔS at 1E+06 Cycles (ksi)			Standard Deviation of Log ΔS (ksi units)		New AISC Classification[6]	Fatigue Crack Initiation Sites[7]
	All R All Sy	R = 0	R = 0 Sy < 50 ksi	R = 0	R = 0 Sy < 50 ksi		
1Q	51.8	51	----	0.074	----	A	----
1H	48.2	45.6	**39.3**	0.06	**0.04**	A	----
1.All	44.9	42.1	**38.2**	0.104	**0.042**	A	----
1M	37.1	36.2	**36.2**	0.04	**0.04**	A	----
8	39.8	39.1	**35.4**	0.094	**0.079**	A	----
2	42.1	41	**35**	0.076	**0.017**	A	----
10(G)	35.2	32.8	**31.6**	0.136	**0.127**	A	Ripple
10Q	31.5	32.7	----	0.114	----	B	Toe
3(G)	31.2	31	**31**	0.084	**0.081**	B	Ripple
1(F)	38.4	38.4	**30.5**	0.117	**0.057**	B (-1)	----
10A	31.1	28.8	**29.7**	0.115	**0.066**	B	Toe
25A	35.8	29.3	**29.6**	0.109	**0.12**	B (-1)	Toe
3	29	29.1	**29.2**	0.049	**0.044**	B	Ripple
13	27.8	27.3	**28.5**	0.055	**0.057**	B (+1)	Toe
28	29.8	28.4	**28.1**	0.097	**0.045**	B	----
12(G)	27.2	27.2	**27.2**	0.072	**0.072**	C	Ripple
10H	35.2	33.1	**25.8**	0.102	**0.101**	C (-1)	Toe
4	27.3	26.8	**25.7**	0.092	**0.095**	C	Ripple
6	27.3	26.8	**25.7**	0.092	**0.095**	C	Ripple
9	25.7	25.8	**25.5**	0.079	**0.085**	C	----
10M	26.4	24.5	**24.5**	0.093	**0.093**	C	Toe
16(G)	22.7	24.5	**24.5**	0.215	**0.215**	C (+1)	Root
25	24.1	23.9	**24.5**	0.09	**0.08**	C(+1)	Toe
7(B)	23.8	23.8	**24.4**	0.083	**0.11**	C (+1)	Toe and C. T.
19	23.2	23.1	----	0.157	----	E?	Toe
30A	23	23	**23**	0.014	**0.014**	D	Toe and D. T.
26	17.4	23	**23**	0.054	**0.054**	D (+1)	Toe
14	25.9	22.9	**22.9**	0.115	**0.109**	D (-1)	Toe
11	22.7	22.7	**22.1**	0.078	**0.08**	D	Toe
21	21.8	21.8	**21.8**	0.117	**0.117**	D	Toe
7(P)	21.5	21.5	----	0.075	----	D	Toe and C. T.
36	20	20	**20**	0.062	**0.062**	D	Toe and D. T.

[6] The shift in AISC category resulting from restricting data base information to R=0 and Sy<50 ksi test results is indicated by +1 or -1 depending upon whether the weldment was increased or decreased by one category.

[7] C.T. = Continuous Termination (wrap-around weld), D.T. = Discontinuous Termination (simple start or stop).

25B	20	20	**20**	0.062	**0.062**	D	Toe or Toe and D. T.
12	19.7	19.7	**19.7**	0.055	**0.055**	D	Toe
16	19.6	19.6	**19.6**	0.104	**0.104**	D	Toe or Root
22	19.1	19.5	**19.4**	0.045	**0.044**	D	Toe
21(3/8")	17.9	17.9	**17.9**	0.037	**0.037**	E	Toe
20	17.5	17.5	**17.5**	0.099	**0.099**	E (+1)	Toe
23	18.3	----	----	----	----	E	Toe
24	18.3	----	----	----	----	E	Toe
30	16.7	16.7	**16.7**	0.051	**0.051**	E	D. T.
38	16	16	**16**	0.058	**0.058**	F	Toe
17A	16.2	15.8	**15.8**	0.051	**0.051**	F	D. T.
17	14.6	14.6	**14.6**	0.046	**0.046**	F	D. T.
18	12.2	12.8	**14.5**	0.107	**0.148**	F (+1)	D. T.
32A	14.1	14.1	**14.1**	0.055	**0.055**	F	D. T.
27	12.8	13.5	**13.5**	0.101	**0.101**	G	----
33	11.6	12.9	**12.9**	0.055	**0.055**	G	Toe at C.T. or D. T.
31A	15.6	15.8	----	0.12	----	F	Toe
46	11.9	----	----	----	----	G	D.T.
40	11.2	----	----	----	----	G	Toe and D. T.
32B	11.2	----	----	----	----	G	Toe and D. T.

Munse and Ang [2] suggested that the effects of scatter on the desired or required reliability of a particular structural detail could be incorporated into the design procedure by calculating a reduction factor (R_F) which shifted the mean curve of a detail's S-N diagram downward by an amount (Fig. 3.2) which would guarantee a desired level of safety (or probability of failure):

$$\Delta S_{design} = \Delta S_{mean} (R_F) \tag{3.1}$$

A relation between the reliability factor (R_F) shown in Fig. 3.2 and the COV[8] of the mean fatigue strength (Ω_S) is given in Eq 3.2 below. A typical values of R_F for a weldment is 0.7.

$$R_F = e^{-2\sqrt{\ln\left(1+\Omega_S^2\right)}} \tag{3.2}$$

Table 3.3 shows that standardizing the data bank information frequently alters the mean fatigue strength (ΔS at 10^6 cycles) and usually reduces the standard deviation in the log of fatigue strength (s) for most structural details. The effects of standardizing the fatigue data bank information on the scatter in the fatigue data for a given detail are plotted in the histograms of Figs. 3.3 and 3.4. As seen in Figs. 3.3 and 3.4, standardizing data banks greatly reduces the scatter in fatigue data for a given detail and consequently increases the allowable design stresses[9].

The scatter in fatigue information is increased by grouping structural details into a small number of broad categories of decreasing fatigue resistance. The AISC weld category fatigue design method [3] and other similar approaches group the data for all strengths of steel, all R

[8] The COV is the coefficient of variation, that is, the percentage of the standard deviation relative to the mean.

[9] Recall that the design stress range (Δ S design) at a certain life (10^6 cycles) can be estimated from the mean fatigue strength (ΔS_{weld}) of a weldment at a given life by: Log ΔS_{design} = Log ΔS_{weld} - 2 s, where s is the standard deviation of Log ΔS.

ratios, and all "similar" structural detail geometry's together into a single data bank for each category. This practice of placing individual structural details into such broad classifications greatly increases the apparent scatter in fatigue data, leads to lower design stresses (Fig. 3.2) , and obscures the effects of many variables which influence the fatigue life of weldments. The data in each of the AISC categories A through F exhibit large scatter and force design stresses 40% or more lower than the mean fatigue strength, that is, this practice results in a reliability factor (R_F) of around 0.4 rather than values of 0.9 to 0.6 which reflect the essential nature of weldments [4]: see Fig. 3.5.

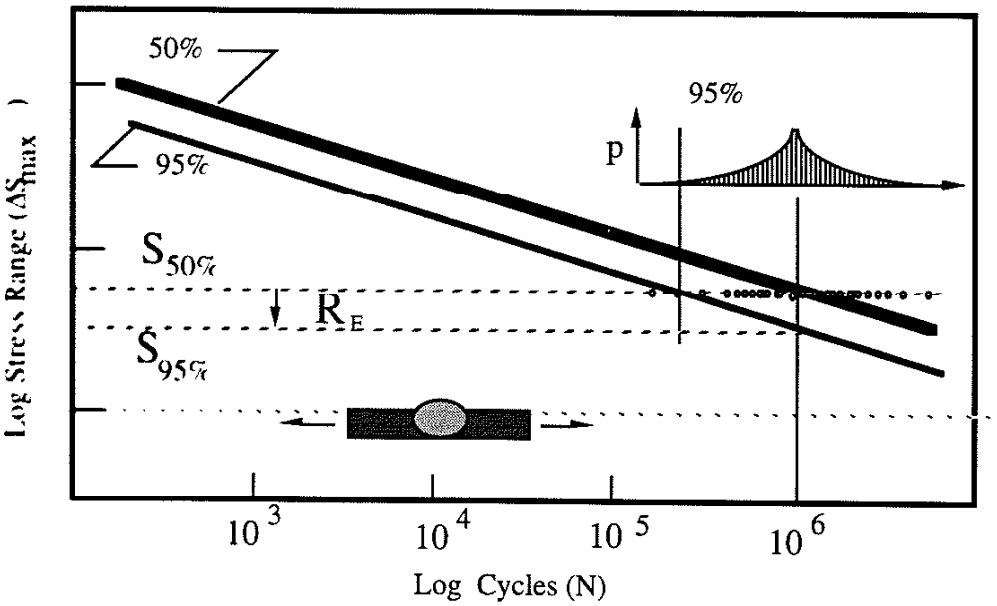

Fig. 3.2 The reliability factor (R_F) is calculated for the desired level of safety given the scatter in the fatigue data for the detail.

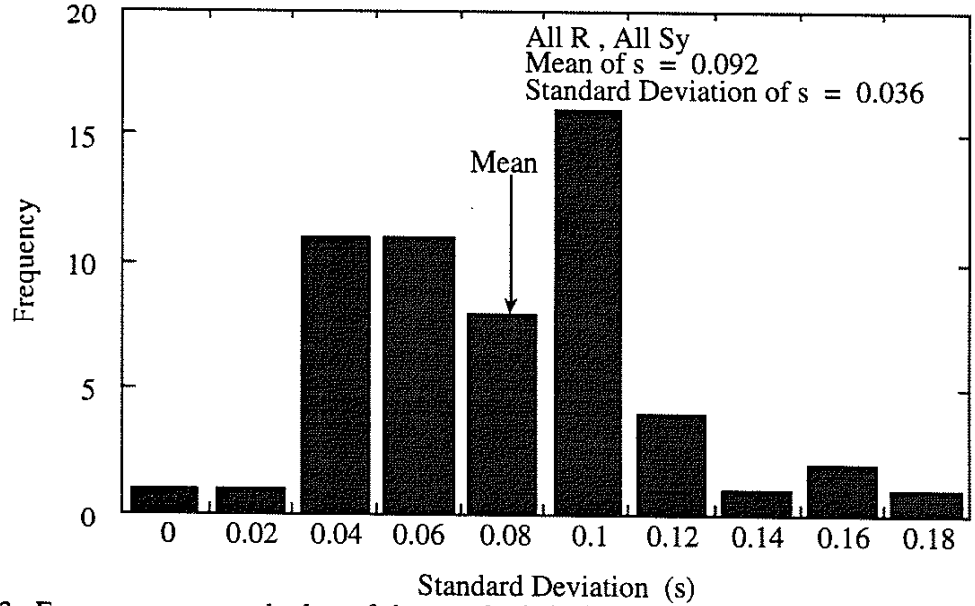

Fig. 3.3 Frequency versus the log of the standard deviation in fatigue strength in MPa: All R ratios and all S_y.

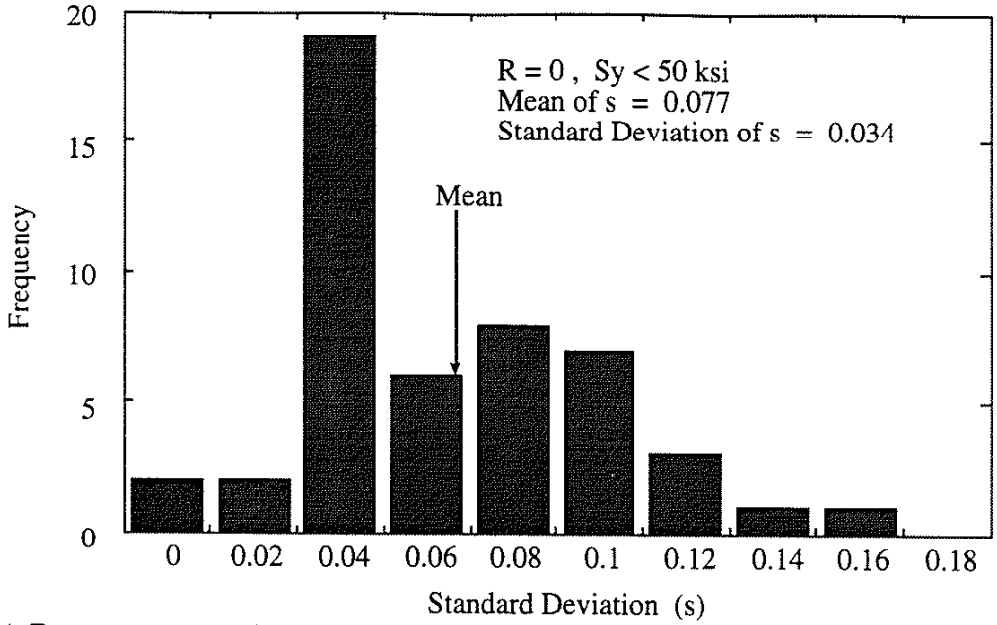

Fig. 3.4 Frequency versus the log of the standard deviation in fatigue strength in MPa: R = 0 and S_y < 50 ksi., only.

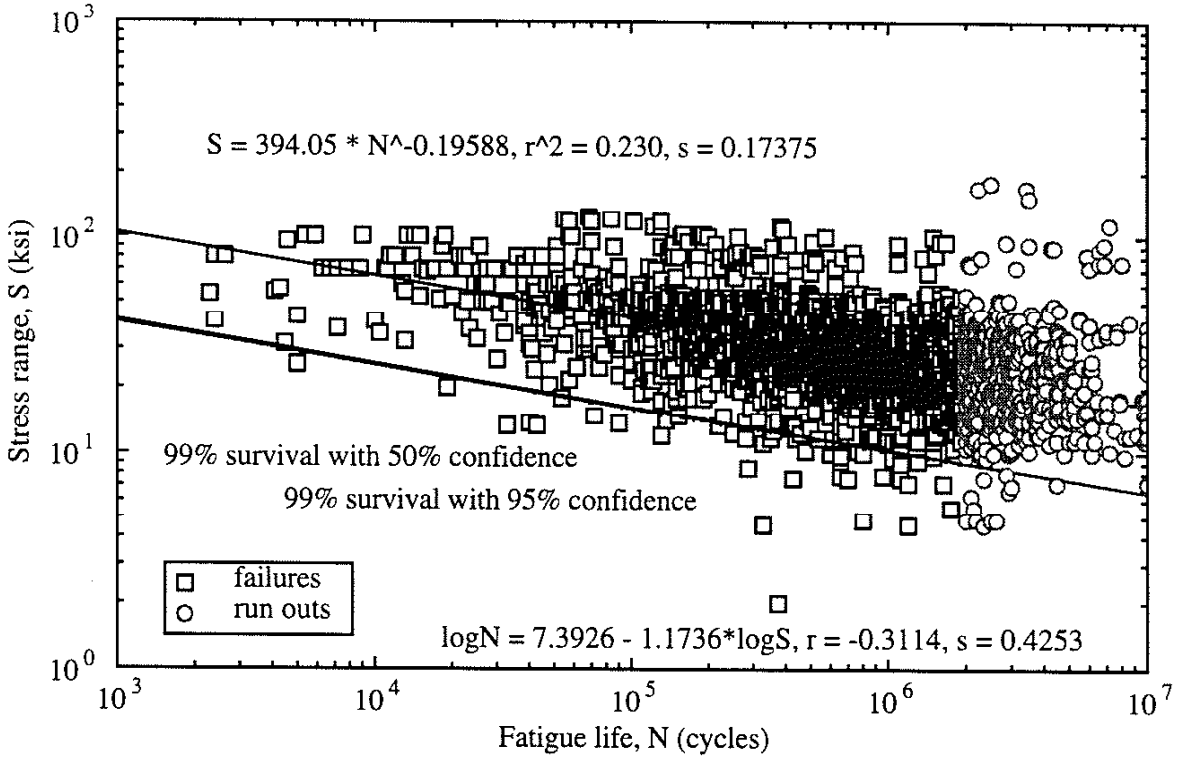

Fig. 3.5 Typical data for AISC Category C weld details. Data taken from the UIUC weldment fatigue data bank. Data for details 7, 10, 11, 12, 13, 14, 19, 22, 23, 24, 25 in Table 3.2. Tests which were discontinued before failure are termed "run outs."

3.4 Classifying Weldment Geometry on the Basis of the Site of Fatigue Crack Initiation

As argued above, eliminating the influence of secondary variables such as R ratio and strength effects gives a sharper picture of true effects of structural detail geometry. A simple way of quantifying the severity of the critical notch in a structural detail is to introduce the concept of the fatigue notch factor (K_f) a nondimensional, scalar quantity which is defined as:

$$K_f = \frac{\Delta S_{\text{smooth specimen}}}{\Delta S_{\text{weldment}}} \approx 1.43 \left(\frac{\Delta S_{\text{plain plate}}}{\Delta S_{\text{weldment}}} \right) \tag{3.3}$$

In the instance of mild steel, K_f can be determined using plain plate data assuming that the fatigue notch factor for plain plate is $K_f = 1.43$. The experimental definition of the fatigue notch factor (K_f) and the use of the mean and standard deviation (s) in design are illustrated in Fig.3.6 below.

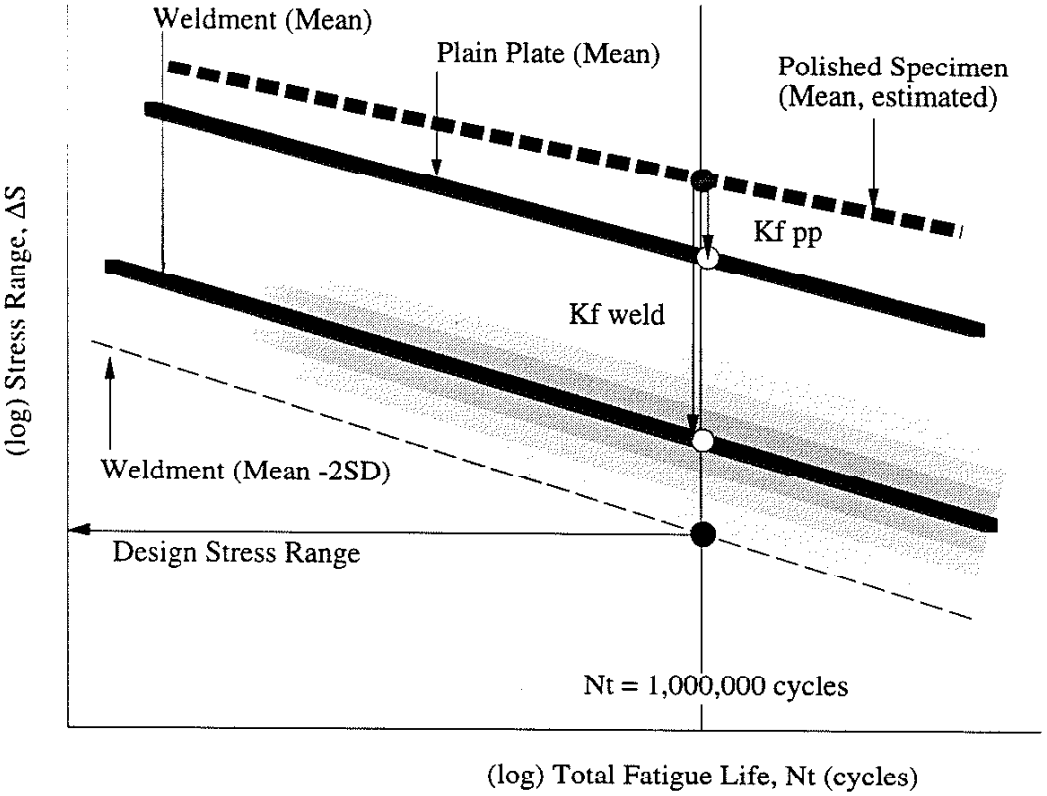

Fig. 3.6 Definition of K_f and the role of the weldment mean strength ($\Delta S_{\text{weldment}}$) and the standard deviation in log of fatigue strength (s) in determining the design stress range permitted for a given service life.

The fatigue behavior of only the welded structural details of Tables 3.2 and 3.3 are reproduced below in Table 3.4. As can be seen, the site at which the fatigue failure initiates in these weldments is inevitably one of four locations: weld ripple, weld toe, weld root, or a weld termination: see Fig 3.7. As seen from the comments in Table 3.4, several weldments are not pure cases of fatigue initiation and growth from either the ripple, toe, root, or termination. These unusual weldments will (for the most part) be eliminated from further consideration and termed

"Mavericks." For instance, all partial penetration welds must be considered mavericks because their fatigue resistance depends entirely on the size of the incomplete joint penetration (IJP) the magnitude of which is generally unknown!

TABLE 3.4. WELDED DETAILS

Details[10]	Loading[11]	Mean Fatigue Strength (ΔS) at 1E+06 cycles (ksi) R=0, Sy < 50 ksi	Standard Deviation of Log ΔS (ksi units)	K_f	New values of ΔS design resulting from "standardizing" the data bank	Fatigue Crack Initiation Sites	Comment
10A	AB	29.7	0.066	1.84	21.9	Toe (G)	
25A	A	29.6	0.12	1.85	17.0	Toe (F)	
3	A	29.2	0.044	1.87	23.8	Ripple	
13*	AB	28.5	0.057	1.92	21.9	Toe	change in flange width
10H	A	25.8	0.101	2.12	16.2	Toe (G)	
4	AB	25.7	0.095	2.13	16.6	Ripple	
6	AB	25.7	0.095	2.13	16.6	Ripple	
10M	A	24.5	0.093	2.23	16.0	Toe (G)	
25	A	24.5	0.08	2.23	16.9	Toe (F)	
07(B)*	AB	24.4	0.11	2.24	14.7	Toe and C. T.	toe or termination failure
26	A	23	0.054	2.38	17.9	Toe (F)	
30A*	B	23	0.014	2.38	21.6	Toe and D. T.	pure bending
14	A	22.9	0.109	2.39	13.9	Toe	
11	AB	22.1	0.08	2.47	15.3	Toe	
21	AB	21.8	0.117	2.51	12.7	Toe	
25B*	A	20	0.062	2.73	15.0	Toe or Toe and D. T.	toe or termination failure
36*	AB	20	0.062	2.73	15.0	Toe and D. T.	toe or termination failure
12*	AB	19.7	0.055	2.77	15.3	Toe	change in flange slope
16*	A	19.6	0.104	2.79	12.1	Toe or Root	partial penetration
22*	AB	19.4	0.044	2.82	15.8	Toe	attachment or cruciform
21(3/8")	AB	17.9	0.037	3.05	15.1	Toe (F')	
20	A	17.5	0.099	3.12	11.1	Toe (F')	
30	A	16.7	0.051	3.27	13.2	Termination	
38*	AB	16	0.058	3.41	12.2	Toe	high restraint
17A	A	15.8	0.051	3.46	12.5	Termination	
17	A	14.6	0.046	3.74	11.8	Termination	
18	A	14.5	0.148	3.77	7.3	Termination	
32A	AB	14.1	0.055	3.87	10.9	Termination	
33	A	12.9	0.055	4.23	10.0	Termination	

Disregarding then the "Mavericks", it is evident in Table 3.4, that weldments initiating fatigue cracks at weld ripple and weld toes have the lowest values of K_f and are the welded details

[10] Those details listed in Table 3.4 with an astericks (*) were labled "Mavericks"

[11] A = Axial, B = Bending, AB = Deep section loaded under bending but stress at hot-spot pseudo-axial.

having the higher fatigue strengths. All weldments failing from terminations are among the worst welded details and have the largest values of K_f and the least fatigue strength[12].

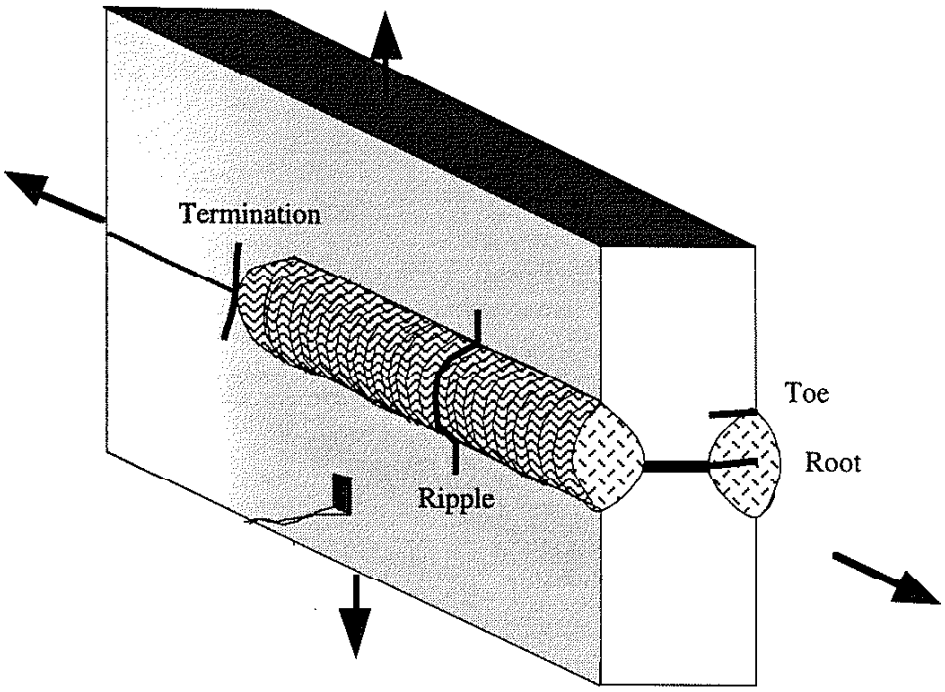

Fig. 3.7 Failure locations in weldments: ripple, toe, root, or weld termination. The distinction between a wrap-around (continuous) termination and a simple termination (stop or start) is not made in this drawing. The Termination and Ripple are sites of fatigue crack initiation only when the load applied to the weldment is longitudinal. Likewise, the Root and Toe become fatigue crack initiation sites under transverse loading. The essential distinctions between these four, fundamentally different inititation sites are summarized in Table 3.5 from a metallurgy and mechanics perspective.

Each of the welded details of Table 3.4 categorized as a "pure" case of fatigue crack initiation from either the weld ripple, weld toe, or weld termination was given the notation:

- **Ripple (R):** Failure initiating from the ripple in a weld.
- **Toe (G)**: Failure initiating from the toe of a groove weld.
- **Toe (F)**: Failure initiating from the toe of either a full penetration load-carrying or any non-load carrying fillet weld.
- **Toe (F')**: Failure initiating from the toe of a partial-penetration, load-carrying fillet weld. This case is actually a "maverick," but it is so important that it is included in the comparisons below.

[12] It should be noted that this weldment has been much studied and is often used as the paradigm for the behavior of all weldments.

- **Termination (T)**: The "start" or "stop" of a fillet or groove weld.

Figures 3.8, 3.9 and 3.10 give schematic diagrams of the weld categories based on sites of fatigue crack inititation and growth.

TABLE 3.5 ESSENTIAL DIFFERENCES BETWEEN RIPPLE, TOE, ROOT, AND TERMINATION FATIGUE CRACK INITIATION SITES

Fatigue crack initiation site	Relevant Fatigue Properties	Notch	Residual stresses
Ripple	WM	Weld ripple: a periodic array of small notches on the surface of the weld bead.	$+S_Y$ WM : No larger than the yield strength of weld metal.
Toe	HAZ	Weld toe: a surface notch having no defined depth and variable notch root radius	$+S_y$ BM: No larger than the yield strength of base metal
Root	(Tempered) WM	Weld Root: a sharp notch having an unknown and variable notch root radius.	Unknown. Probably near zero if the fit-up is not tight.
Termination	HAZ	Weld toe: As above except it is possible or even probable that starts will involve a lack of fusion and stops may involve crater cracks, pipes or hot cracks.	$\pm S_Y$ WM : Possibly as high as the yield strength of weld metal?

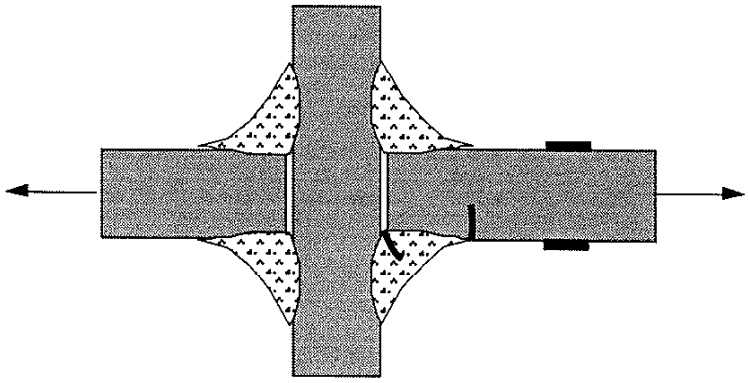

Toe (F'): Load-Carrying Cruciform joint

Fig. 3.8 A "Maverick." The load carrying fillet weld is an important case. Failure may occur at either the weld toe or weld root. Applied axial stresses favor root failures. Applied bending stresses favor toe failures. The size of the IJP controls the notch severity (K_f) of both the root and the toe with the result that this weld can be as "good" as a "good" weld or as "bad" as a termination depending entirely upon the size of the IJP.

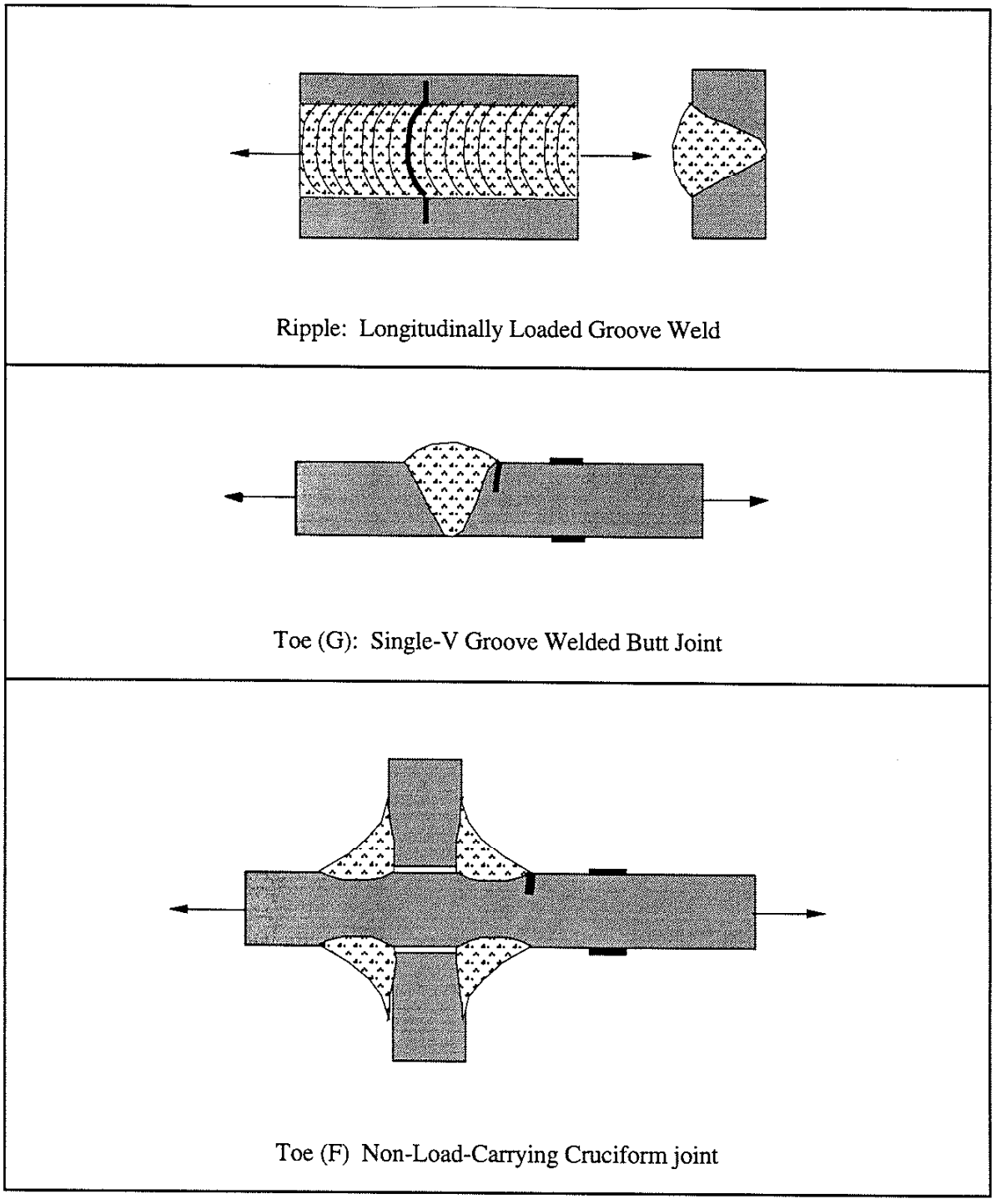

Fig. 3.9 The "Good" welds. Initiation site at a weld ripple or a weld toe.

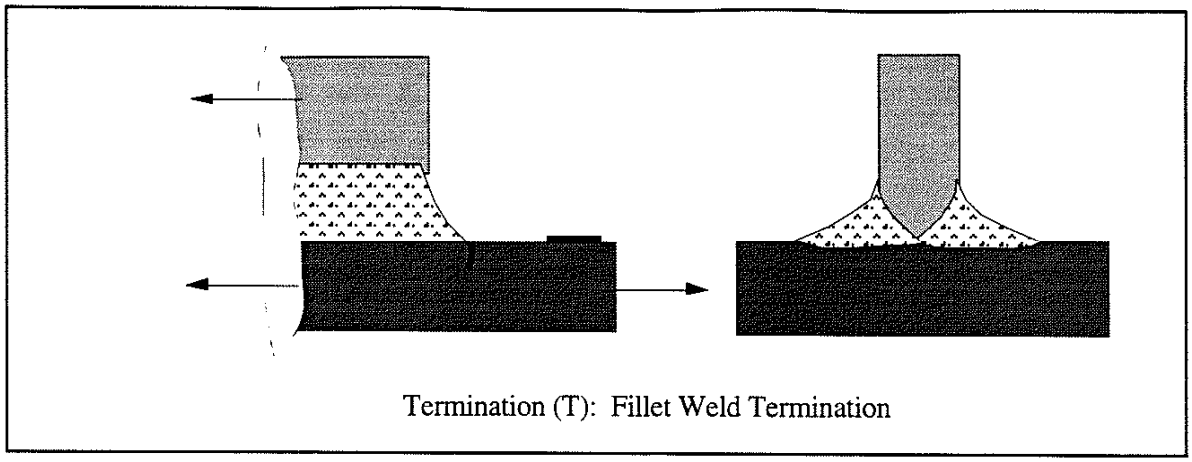

Fig. 3.10 The "Bad" weld. Initiation site at the end of a fillet weld.

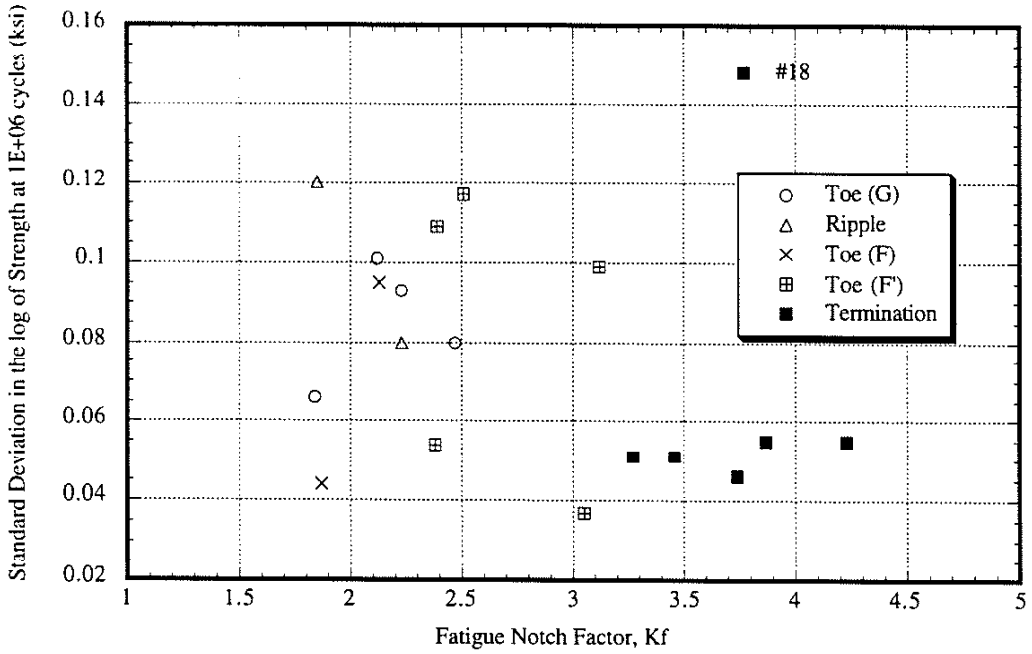

Fig. 3.11 Variation in the log of the standard deviation in fatigue strength in ksi (s) with fatigue notch factor (K_f). The uncertainty in the fatigue strength of terminations would seem to be generally less than that of the toe and ripple.

The effect of this system of categorizing weldments is shown in Figs 3.11 and 3.12. In Fig. 3.11 the standard deviation of the log of strength (s, ksi units) is plotted versus K_f for each of the details listed in Table 3.6. Several interesting observations can be made. First the scatter in fatigue strength is inversely related to K_f. The welds having a higher fatigue resistance exhibit more scatter presumably because fatigue crack initiation plays a larger role. On the other hand, weld having the lowest fatigue resistance have less scatter in their fatigue data presumably because their behavior is governed entirely by fatigue crack growth. Secondly, it is obvious that weldments for which fatigue cracks initiate at the ripple or toe have relatively small values of K_f

(1.8 to 2.5); whereas, terminations have very high values of K_f (3.0 to 4.5). The "Maverick" load-carrying cruciform is seen to range in behavior from as bad as the terminations to as good as a non-load carrying cruciform weldment.

These observations are reinforced by the S-N diagrams of Fig. 3.12. It is interesting to note that the slopes of the S-N diagrams for the terminations are different from the slopes for the ripple and toe categories. The slope of the S-N diagrams for the terminations portrays a situation in which there is very little if any contribution from crack nucleation (N_N) and early crack growth (N_{P1}) or at least no crack closure: in such a case the slope of the S-N diagram is -1/n or -1/3 for mild (ferritic-pearlitic) steel. The more nearly horizontal slope for the ripple and toe category welds indicates a substantial crack nucleation (N_N) and early crack growth (N_{P1}) contribution to their total life. The slopes of S-N diagrams are an incontrovertible indication of the importance or unimportance of crack nucleation and early crack growth.

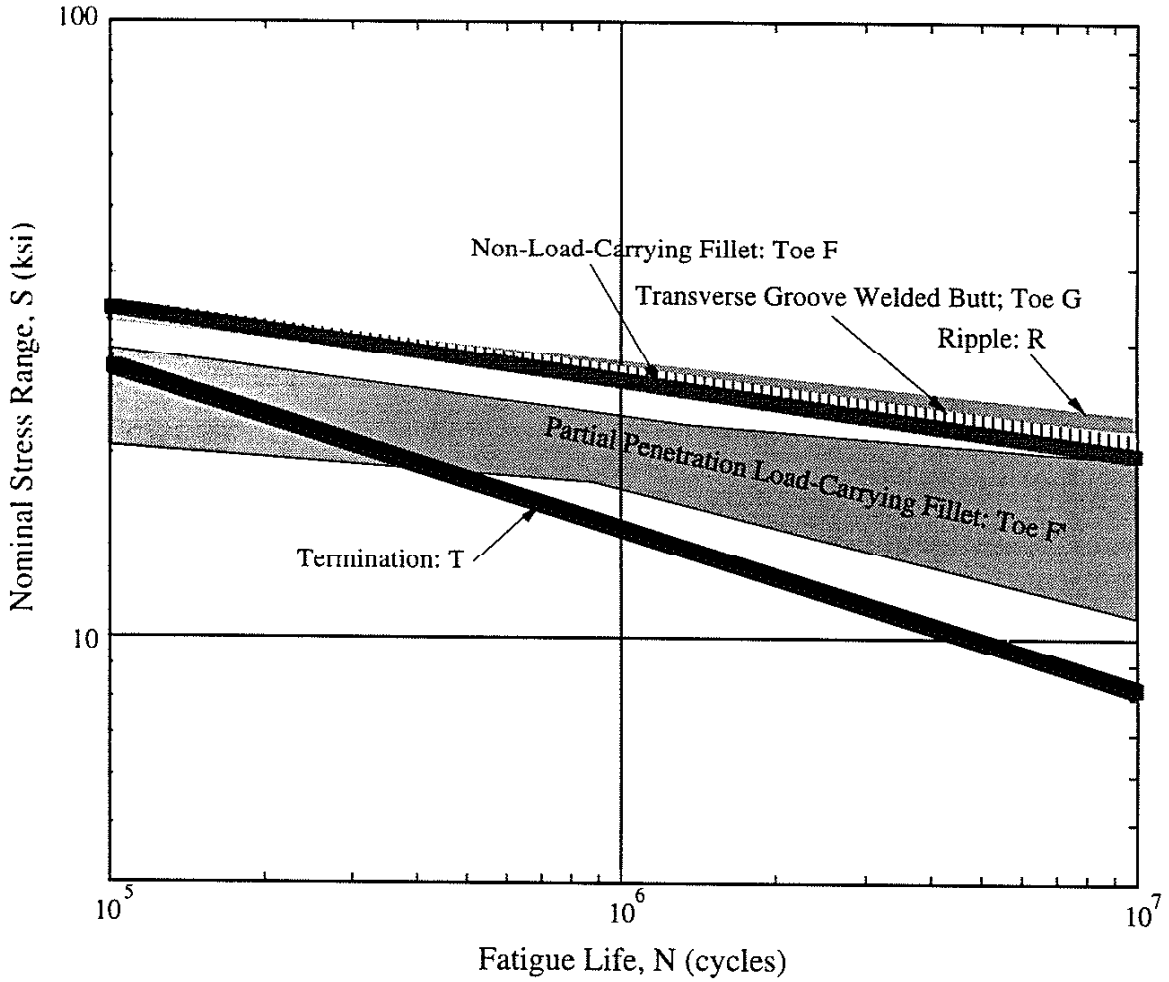

Fig. 3.12 Average S-N diagrams for the welded details in Table 3.6. The average S-N curves for Ripple, (R), Toe (G) and Toe (F) are similar. The fatigue behavior of the "Maverick" Toe (F') - partial penetration load carry fillet - ranges from being as bad as the terminations to as good as the Toe (G and Toe (F) data.

3.5 Summary

Joint geometry has a large influence on the fatigue resistance of weldments. While it is an appealing idea to assemble the fatigue data for weldments into a comprehensive "encyclopedia" organized to reflect their fatigue behavior, such efforts are doomed because there are just too many different joint geometries. If one classifies weldments by the site of fatigue crack initiation, it would seem that there are "Good" weldments for which fatigue cracks initiate at the weld toe or weld ripple, "Bad" weldments which are substantially worse than "Good" weldments for a variety of reasons, and finally "Mavericks" of which the fatigue resistance depends largely upon the undefined size of a discontinuity or is complicated by an ambiguity as to the definition of nominal stress.

Collecting weldment fatigue data into a limited number of broad weld "Categories" is an appealingly simple concept and thus useful for designers, but this practice increases the apparent scatter in weldment fatigue data and reduces the allowable design stresses for a required level of safety. The scatter in both the encyclopedia approach and the weld category approach inevitably obscures the effects of the secondary but nonetheless important fatigue variables.

In the next chapter, the variables influencing the fatigue resistance of an individual joint geometry, a non-load-carrying cruciform weldment, will be investigated with the aid of a computer simulation of weldment fatigue behavior. This weld geometry will be taken as a paradigm for the fatigue behavior of weldments which initiate fatigue failure at a weld toe, that is, "Good" weldments. The behavior of "Nominal" and "Ideal" weldments, that is, non-load-carrying cruciform weldments with and without a 0.1-in. weld discontinuity at the weld toe, will be compared and contrasted.

4. Variables Effecting the Fatigue Life of an Individual Weldment

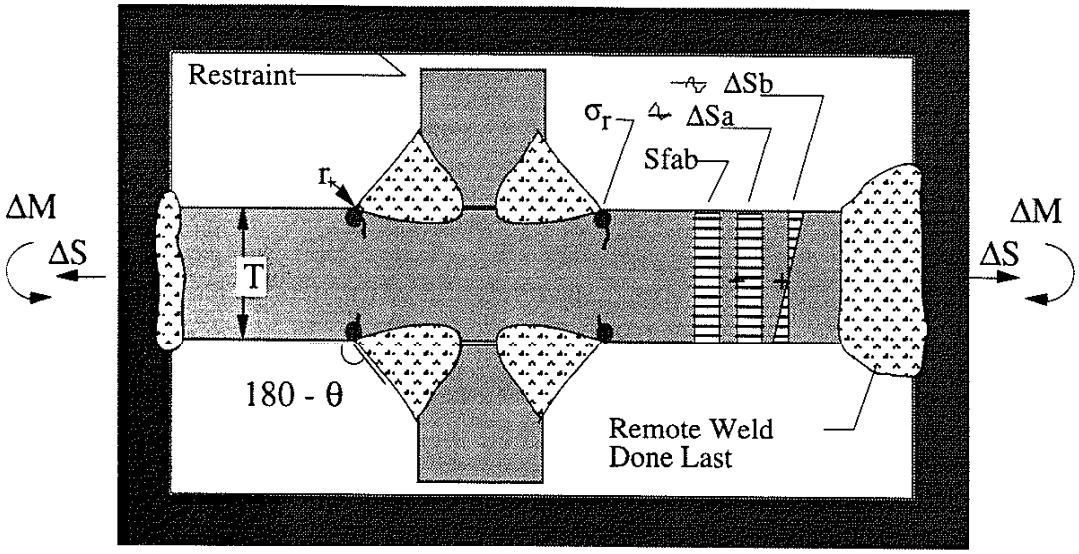

Fig. 4.1 Schematic diagram of a non-load-carrying cruciform weldment subjected to axial and bending loads as well as to global residual (mean) stresses generated by subsequent welding fabrication (S_{fab}). Welding residuals (σ_r) are considered to exist only at in a small volume at the weld toe.

4.1 The Variables Effecting Weldment Fatigue Behavior

The variables influencing the fatigue life of a non-load carrying cruciform weldment (Fig. 4.1) are:

- **Applied stress amplitude**: The remote axial and bending stresses (ΔS_A and ΔS_B) referred to the the station of the weld toe. The bending stresses may be applied or secondary stresses resulting from weld fabrication distortions[13].
- **Mean and residual stresses**: Remote mean stresses resulting from the applied loads (S_m), welding residual stress at the weld toe (σ_r), and fabrication residual stresses resulting from subsequent remote welding (S_{fab}) which add to the remote mean stresses.
- **Material properties:** Strain controlled fatigue properties (ε'_f, σ'_f, b, c) determine the resistance to crack nucleation and early crack growth, while the crack growth properties (C, m) control the growth of fatigue cracks. The residual stresses are limited (often controlled by) the metal's yield strength (S_y) and so yield strength of the weldment's constituent materials is of great importance in non-stress-relieved weldments.
- **Geometrical stress concentration effects:** The concentration of stress and strain at a notch such as a weld toe magnify the effects of the applied stress, the remote mean stress and the fabrication stresses. Thus notches reduce the fatigue life, particularly N_N and N_{PI}. The effects of the notch are captured by the fatigue notch factor (K_f) which influences N_N and N_{PI} and by M_k which is the elevation of the range in stress intensity factor at the weld toe.

[13] Welding distortions may not induce secondary bending stresses when the applied load is pure bending.

- **Size and location of welding discontinuities:** The weld discontinuities both at the notch root and elsewhere magnify the stress concentrating effects of the critical notch and can greatly reduce N_N and N_{P1}, and N_{P2}. The presence of a 0.1-in. planar discontinuity at the weld toe of the non-load-carrying cruciform weldment considered here is the condition which distinguishes the "Nominal" from the "Ideal" weldment.

4.2 The Role of Analytical Models

The fatigue of weldments is a complicated topic! No two weldments are identical; and weldment fatigue resistance depends upon many variables in a complex, non-linear way. The effects of the major variables such as stress range and weld geometry are certainly understood; and one can usually predict what will happen if one of these major variables is changed; however, it is difficult to predict what will happen if these and several secondary variables are changed at once; in such a circumstance, the outcome may be counterintuitive.

Computer models can simulate the behavior of such complex, non-linear systems. Fracture mechanics crack growth models for N_{P2} provide the lower bound estimates of N_{P2} for the "Nominal" weldment; while the I-P model described below which combines the LEFM model estimates of N_{P2} (the crack propagation life or "P") with estimates of N_N and N_{P1} (crack initiation life or "I") can provide estimates the upper bound behavior of the "Ideal" weldment [5].

$$N_T = [N_N + N_{P1}] + N_{P2} = N_I + N_{P2}. \quad (4.1)$$

TABLE 4.1 MATERIAL PROPERTIES USED IN ESTIMATING WELDMENT FATIGUE LIFE

Source	Property, symbol (units)	A36 HAZ	A514 HAZ
Tensile Properties	Ultimate Strength, S_u (ksi.)	97	204
	Yield Strength, S_y (ksi.)	77	171
	Base Metal Yield Strength, S_{yBM} (ksi.)	35	100
	Young's Modulus, E (ksi.)	2.74e+04	3.03e+04
	Peterson's Constant, a_p (in.)	0.01	0.005
	Monotonic Strength Coefficient, K (ksi.)	142	306.0
Strain-Controlled Fatigue Properties	Cyclic Strength Coefficient, K' (ksi.)	216	256.0
	Monotonic Strength Exponent, n	0.102	0.092
	Cyclic Strength Exponent, n'	0.215	0.103
	Cyclic Ductility Coefficient, ε_f'	0.218	0.783
	Cyclic Strength Coefficient, σ_f' (ksi.)	105	290
	Cyclic Strength Exponent, b	-0.066	-0.087
	Cyclic Ductility Exponent, c	-0.492	-0.713
Crack Growth Properties	Paris C, (in./cycle)	3.6e-10	6.6.e-09
	Paris C', (in./cycle)	1.21e-09	1.64e-08
	Paris Exponent, m_p	3.0	2.25
	Fracture Toughness, K_{IC} (ksi$\sqrt{in}$)	100	150

4.3 The Initiation-Propagation Model

Figure 4.2 shows the organization of the Initiation-Propagation (I-P) model. The unshaded parts of Fig. 4.2 are results from prior experiment and analysis which are presumed to be available: strain controlled fatigue properties, crack growth properties, tensile properties, and a careful (FEM) stress analysis of the weld joint geometry. The material properties used in this work are listed in Table 4.1. The I-P model predicts the total fatigue life of a weldment (N_T) by making separate estimates of the fatigue crack initiation life (N_I) and the fatigue crack propagation life (N_{P2}) and summing them.

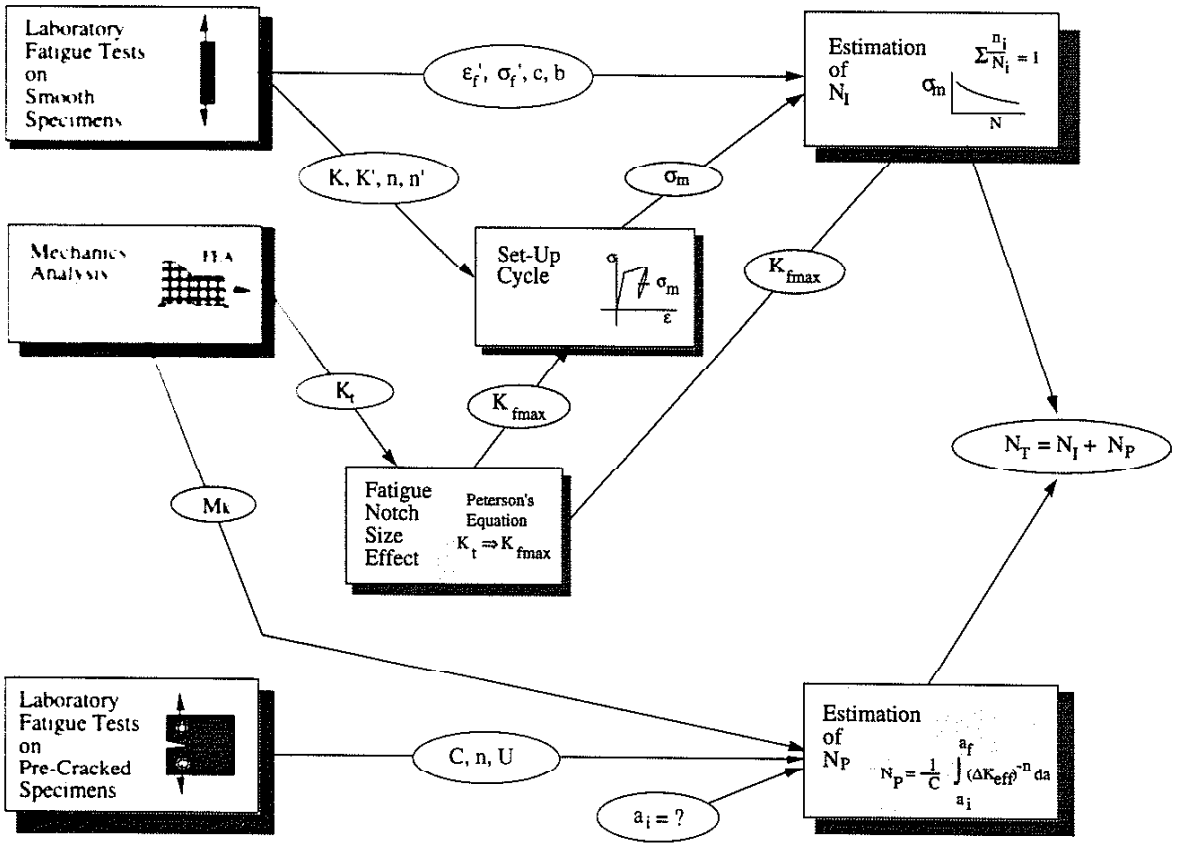

Fig. 4.2 A schematic diagram showing the information required by and the organization of the I-P model

The fatigue crack initiation life (N_I) is thought of as the life period spent in crack nucleation and the growth of small cracks through (roughly) the first 50μm - 100μm of the metal, that is, N_N and N_{PI}. This life period is captured in the fatigue behavior of smooth specimens, and thus, strain-controlled fatigue life concepts are used to estimate this life period. The severity of the notch presented by the weld toe is quantified using the K_{fmax} hypothesis, a concept for determining the pessimum value of fatigue notch factor K_f using Peterson's Equation.

A second noteworthy feature of the N_I part of the I-P model is the use of the "Set-Up Cycle" analysis to determine the notch-root mean stress remaining after the first few cycles. This analysis approximates the effects of notch-root plasticity during the first few applications of load through the use of Neuber's Rule and models the difference in behavior between monotonic (first reversal) and cyclic (subsequent reversals) behavior of the material at the notch root (the grain-coarsened HAZ). This phenomenon is called the Bauschinger effect. The first reversal includes

the effects of the initial loading from 0 to S_{max}, the weld toe (welding) residual stresses (σ_r)[14], and the remote fabrication stresses (S_{fab}). The "Set-Up Cycle" analysis provides the initial value of notch root mean stress for the linear cumulative damage calculation which considers the exponential decay of the notch-root mean stress during subsequent cycling. Thus, N_I is calculated considering the notch-root mean stresses established during the first few cycles of load application and their relaxation during the fatigue crack initiation period.

The calculation of N_{P2} is based on ΔK_{eff} and values for the effective stress intensity ratio (U). The M_k value in [6] was used. The R ratio is redefined for the estimation of the N_P: the notch-root mean stresses are not considered because they exist only in the small volume of material at the notch root; furthermore, in most cases, the I-P model predicts that these notch-root mean stresses substantially diminish during the crack initiation period. Therefore, only the applied mean stresses and the mean stresses resulting from subsequent fabrication (S_{fab}) are assumed to influence crack growth. Crack shape development [7] is included. For "Ideal" weldments, the initial crack size is arbitrarily taken as $a_i = 0.01$ inches. The final crack size (a_f) was determined using LEFM and K_{IC}.

For the "Nominal" weldment, N_I was neglected and N_{P2} was calculated assuming an initial flaw size $a_i = 0.1$ in.

4.4 Validation of the I-P Model

Figures 4.3 to 4.6 show experimental data form the UIUC fatigue data bank for a butt joint (#10) and non-load carrying cruciform weldments (#25) for R = 0 and R = -1 test conditions. In each figure, the predictions of the I-P model for the "Ideal" and "Nominal" weldments are seen to bound the experimental data[15].

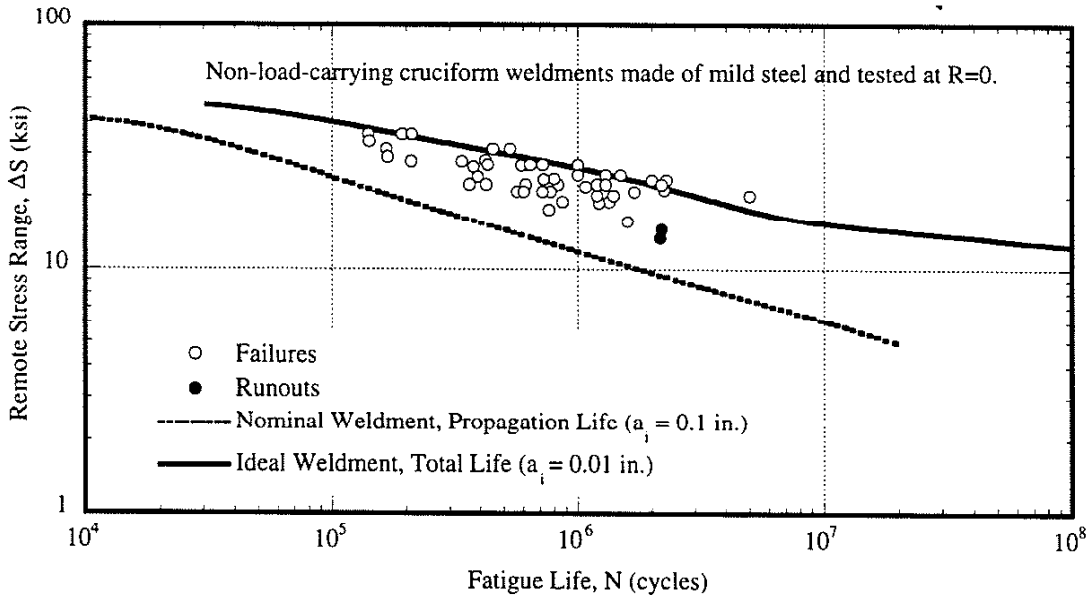

Fig. 4.3 Comparison of the predictions of the I-P model with data in the UIUC weldment fatigue data base for a mild steel non-load-carrying cruciform weldment , R = 0.

[14] In the "Set-Up Cycle" simulation, the notch-root (welding) residual stresses are treated as an equivalent remote stress by dividing the notch root residuals stresses by K_{fmax}.

[15] When propagation dominates, the slope of the S-N curve is 1/n or 1/3. When initiation dominates, the slope of the S-N curve is 1/b or around 1/8 to 1/10. Thus, the slope of theoretical and experimental S-N curves reflect the relative importance of "I" and "P".

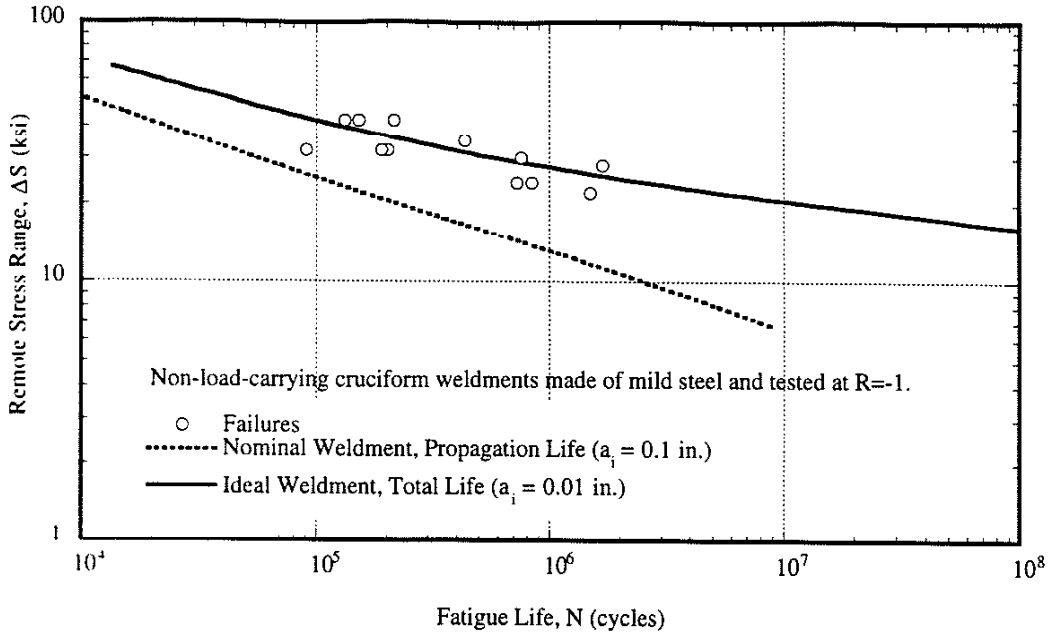

Fig.4.4 Comparison of the predictions of the I-P model with data in the UIUC weldment fatigue data base for a mild steel non-load-carrying cruciform weldment , R = -1.

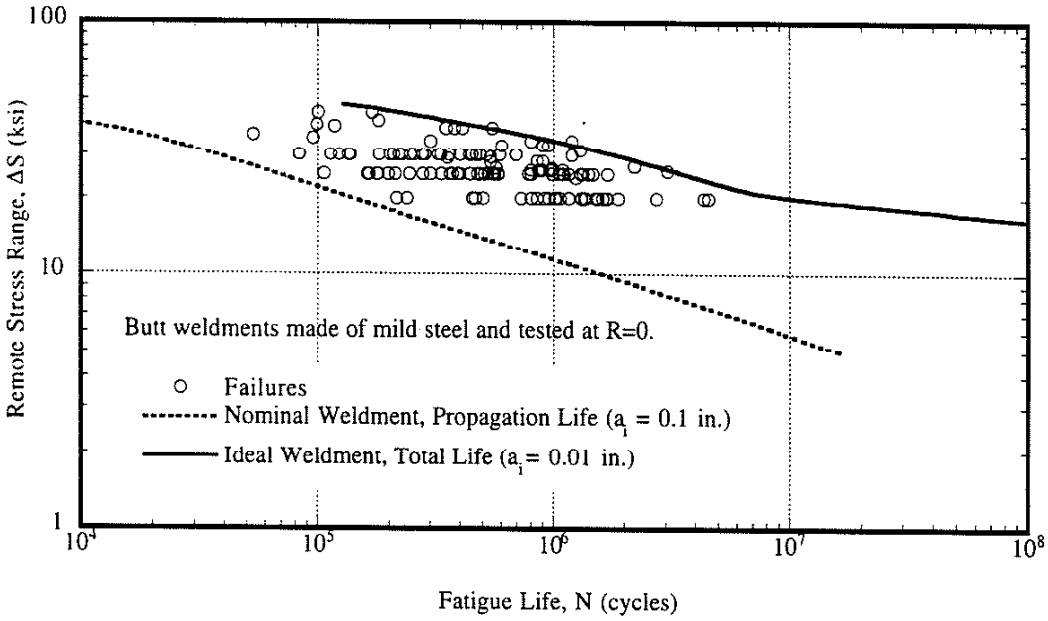

Fig. 4.5 Comparison of the predictions of the I-P model with data in the UIUC weldment fatigue data base for a mild steel double-V butt weldment , R = 0.

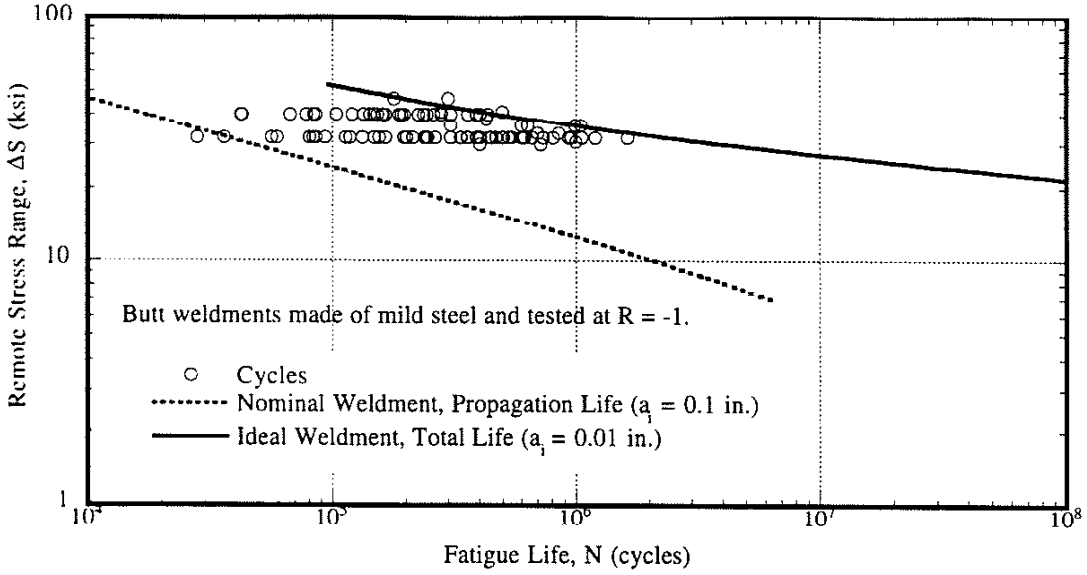

Fig. 4.6 Comparison of the predictions of the I-P model with data in the UIUC weldment fatigue data base for a mild steel double-V butt weldment , R = -1.

4.5 The Effect of Residual Stresses

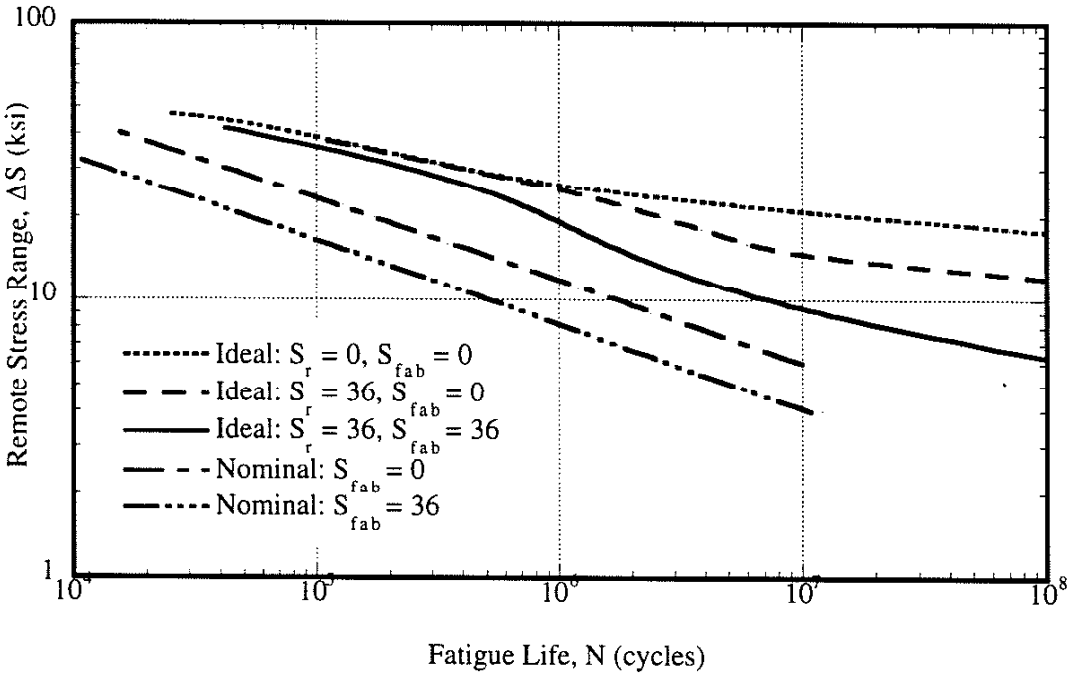

Fig. 4.7 Effect of residual stresses on the fatigue behavior of "Nominal" and "Ideal" 1.0-in plate thickness, mild-steel, non-load carrying cruciform weldments.

Residual stresses greatly influence the fatigue life of both the "Nominal" and "Ideal" weldments as shown in Fig. 4.7. In Fig. 4.7, the welding residual stresses (σ_r) and the fabrication

stresses (S_{fab}) were presumed to be either 0 or their largest possible value, the yield strength of base metal (36 ksi.). Both N_I and N_P are much affected by fabrication stresses. As can be seen, there is a very large difference between the total lives of both "Nominal" and "Ideal" weldments with and without fabrication stresses. This effect is probably a major source of the reported large difference between fatigue tests using small, simple testpieces and full-scale fatigue tests on complex welded structures in which large fabrication stresses (S_{fab}) exist.

4.6 The Effect of Weldment Size

The effect of weldment size is a subject of continuing controversy. The predicted effect of size on the fatigue strength at 10^7 cycles is shown for both the "Nominal" and "Ideal" weldment in Fig. 4.8. The predicted behavior of the "Ideal" weldment is similar to the currently anticipated size effect and has a slope of ≈ -1/3. Note that "Ideal" weldments with high fabrication stresses may have a slope greater than -1/3. The 0.1-in discontinuity in the "Nominal" weldment leads to essentially no size effect for weldments having T > 1.0 in. and an unexpected reversal in the size effect when T < 0.7 in.

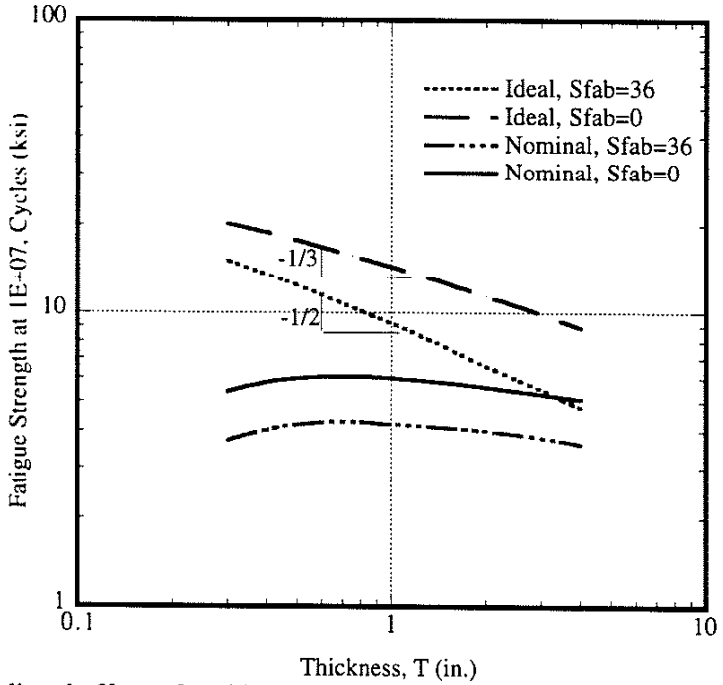

Fig. 4.8 The predicted effect of weldment size for both a "Nominal" and "Ideal" mild steel non-load-carrying cruciform weldment.

4.7 The Effect of Material Properties

The fatigue strength of a mild steel (S_y = 36 ksi) and a quenched and tempered steel (S_y = 100 ksi) are compared in Fig. 4.9 below. To a first approximation, the most important change in material properties is a increase in the yield strength (S_y). High strength materials can sustain much more damaging welding and fabrication residual stresses. So any improvement in fatigue resistance resulting from increasing the strength of a material is usually more that offset by the level of tensile residual stresses which develop during fabrication. If one can induce compressive residual stresses or reduce the size of the as-welded, tensile residual stresses, the fatigue strength of higher strength "Ideal" weldments of high strength materials can be much improved. The Q&T steels perform better when the residual stresses are small or compressive and when crack growth is relatively unimportant, that is, for small-thickness, "Ideal" weldments.

4.8 Effectiveness of Fatigue Life Improvement Measures

There are essentially two strategies for improving weldment fatigue strength: alter the residual stresses or improve the stress-concentrating geometry of the critical notch (weld toe) or a combination of both. In Figs. 4.10 and 4.11, the predicted effect of various fatigue strength improvement measures on the fatigue strength of "Ideal" and "Nominal" mild steel non-load carrying cruciform weldments is shown . The fatigue strength of "Ideal" weldment can be much improved; whereas, that of "Nominal" weldments cannot.

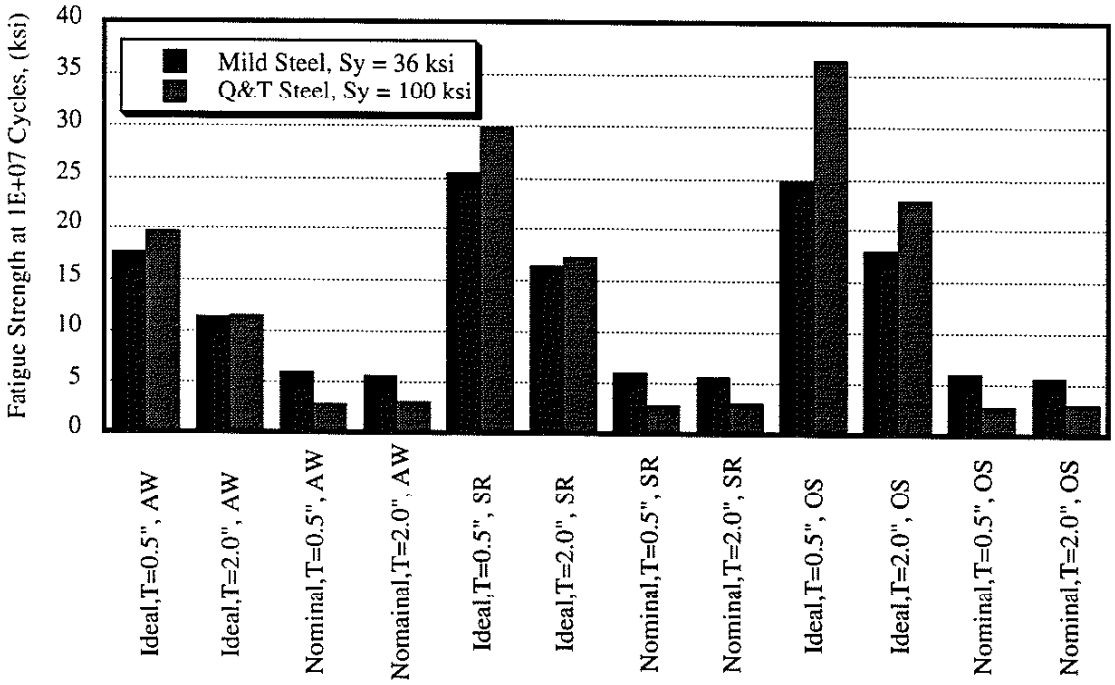

Fig. 4.9 Effect of material properties on the fatigue strength of non-load carrying cruciform weldments under R = 0 loading. For the purposes of this comparison S_{fab} is presumed to be 0. AW = as welded; SR = stress relieved; OS = overstressed in tension.

4.9 The Combined Effect of Weldment Size and Fabrication Stresses on "Nominal" and "Ideal" Weldments

Weldments or welding applications could be categorized according to weldment size and weld quality:

- **light industry applications** in which the weldment size is about 0.5-in or less. For such weldments it is presumed that the weldments are "simple" and do not therefore engender high fabrication stresses, that is, $S_{fab} \approx 0$.
- **heavy industry applications** in which the weldment size is about 2.0-in. It is presumed that the weldments are "complex" and therefore do engender high fabrication stresses, that is, $S_{fab} \approx +S_{yBM}$.
- **high quality welding processes** such as GTAW and GMAW in which the weld perfection may approach that of the ideal weldment.
- **low quality welding processes** such as SMAW in which the weld perfection is low and a substantial initial weld discontinuity must be assumed present. Such weldments may approach the behavior of the "Nominal" weldment ($a_i \approx 0.1$-in.).

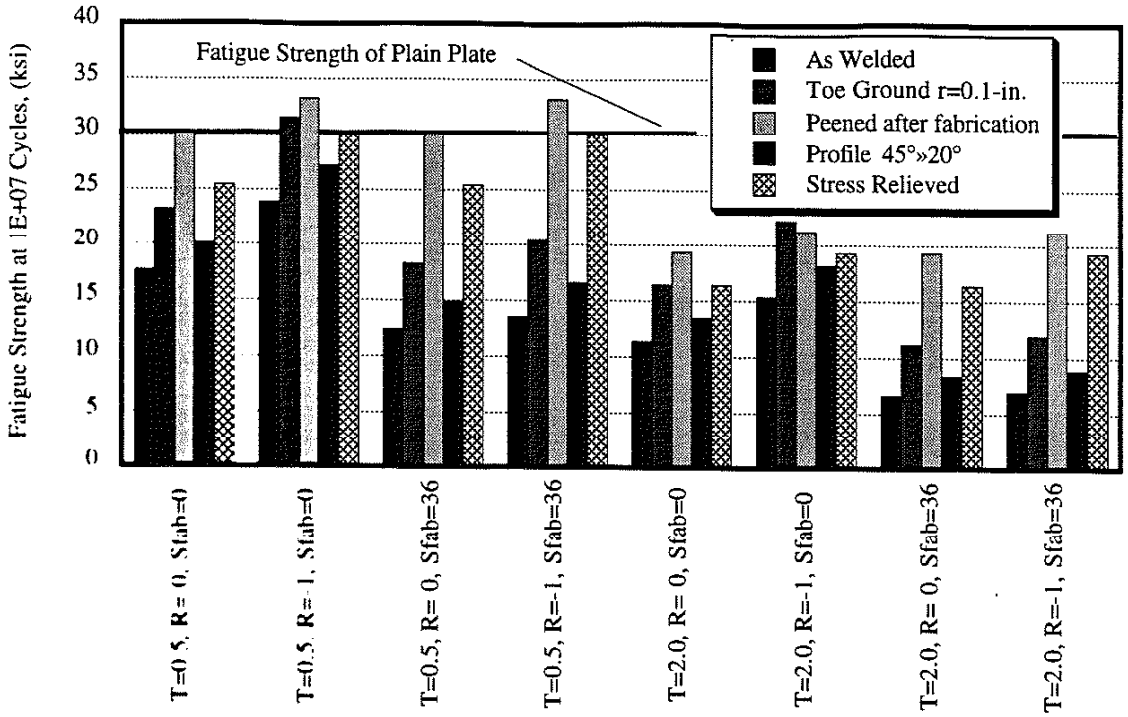

Fig. 4.10 The predicted effect of various fatigue strength improvement treatments on the fatigue strength of a "Ideal" mild-steel, non-load-carrying cruciform weldment, R=0. Some improvement techniques can cause the weldment to equal the fatigue strength of plain plate which because of its rolled-in surface discontinuities has a $K_f \approx 1.43$ [8].

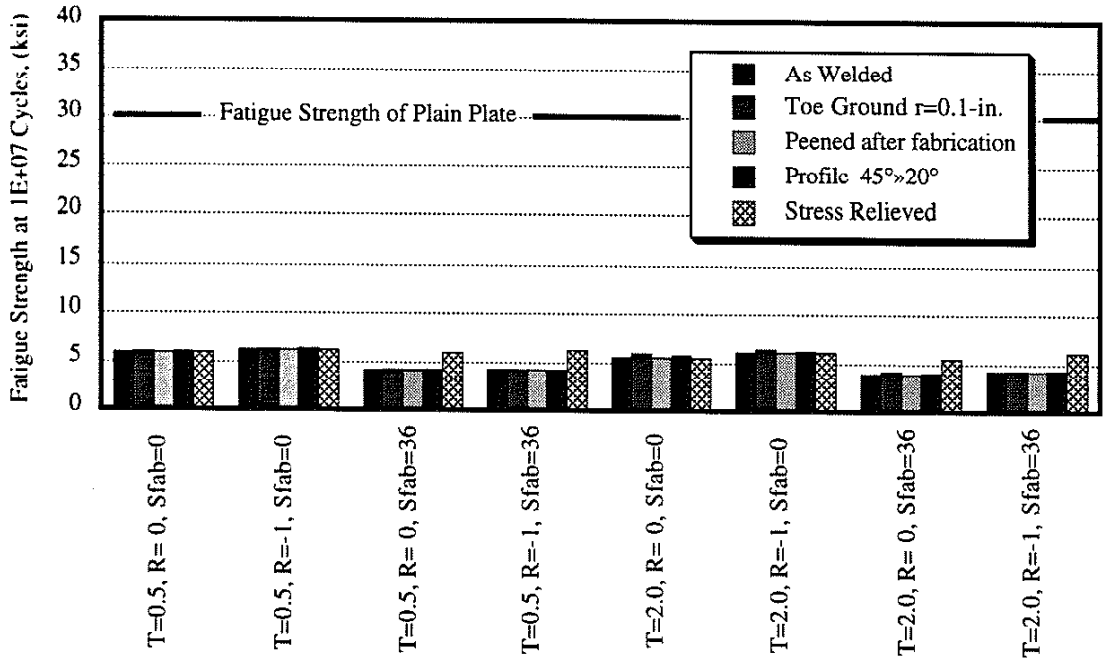

Fig. 4.11 The predicted effect of various fatigue strength improvement treatments on the fatigue strength of a "Nominal" mild-steel, non-load-carrying cruciform weldment, R=0.

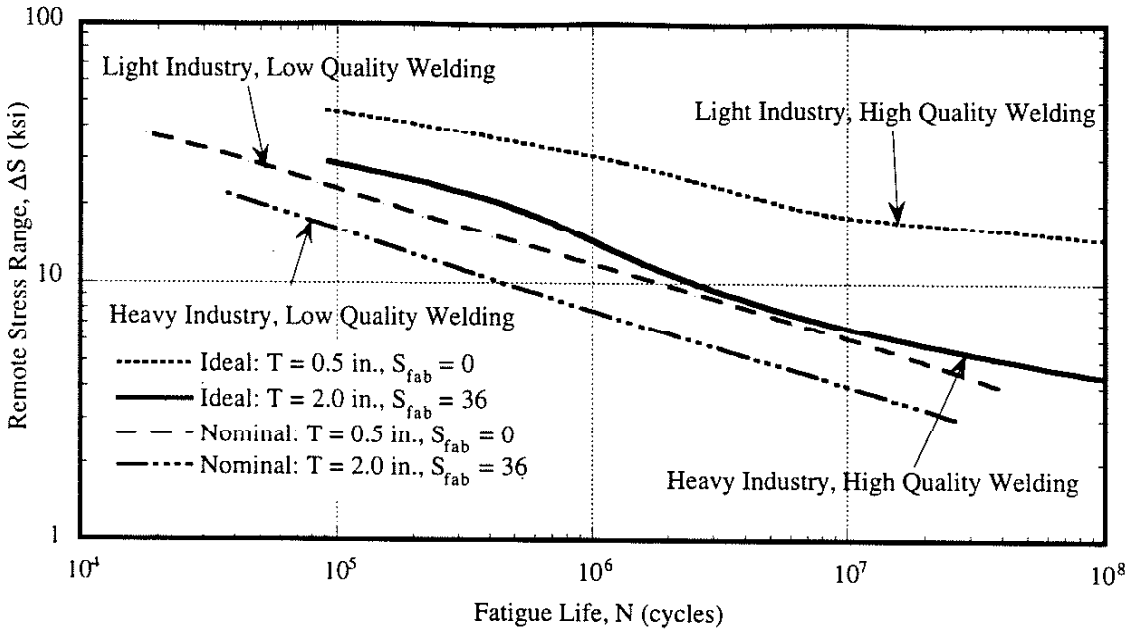

Fig. 4.12 Comparison of four hypothetical cases: Light Industry-High Quality Welding, Light Industry-Low Quality Welding, Heavy Industry-High Quality Welding, Heavy Industry-Low Quality Welding. Mild steel cruciform weldments R = 0. The small-size, high-welding quality weldments typical of the ground vehicle industry may perform substantially better than larger and more complex, or lesser quality weldments.

4.10 Modeling the Uncertainty in Weldment Fatigue Strength

In Chapter 3, it was seen that the scatter or uncertainty in weldment fatigue data overshadowed the effect of most of the fatigue variables discussed in this chapter. While these variables may have only a moderate effect on the mean fatigue life, they are the source of scatter in the fatigue strength data for a given weldment; and as seen in Chapter 3, this scatter forces low design stresses to avoid frequent failures.

A powerful application of the analytical models employed here to estimate the mean fatigue life or strength of a given weldment is to use the model as the basis of a stochastic analysis of weldment fatigue life and to imagine that some or all of the variables considered by the model are stochastic in nature. In this way, the uncertainty in the fatigue resistance of a weldment can be estimated, and the contribution of each fatigue variable to the total uncertainty in fatigue strength of a weldment can be assessed.

The uncertainty in the fatigue life of the "Nominal" weldment has been studied by Engesvik and Moan [9]. For weldments with large welding discontinuities, the major sources of scatter in fatigue data are variation in the size of the weld discontinuity and in the magnitude of the fabrication stresses.

In contrast, the uncertainty in the fatigue life of the "Ideal" weldment depends upon a large number of variables. Lawrence and Chang [8] suggested an simple, approximate expression based on the Basquin-Morrow Equation for the fatigue strength of a weldment at long lives which assumed that at long lives $N_T \approx N_N + N_{P2}$ that is $\approx N_I$:

$$S_a^T = \frac{(\sigma_f' - \sigma_r)\,(2N_I)^b}{K_{f\,max}^{eff}\left(1 + \frac{1 + R}{1 - R}(2N_I)^b\right)} \tag{4.2}$$

Equation 4.2 was factored to isolate five important attributes of weldments which determine their fatigue strength: the notch severity of the discontinuity (G); the mechanical properties of the material in which fatigue crack initiation and short crack growth takes place (P); the applied mean stresses effects (MS); the residual stresses resulting from fabrication and subsequent use of the weldments (RS) and the self-induced stresses caused by the welding distortions (B). Equation 4.2 was rewritten assuming that the weldments are axially loaded and the bending stress components are induced by the welding distortions [4]:

$$S_a^A = P \bullet G \bullet B \bullet RS \bullet MS \bullet (2N_I)^b \tag{4.3}$$

where:

$P = \sigma_f'$ — Effects of Material Properties

$G = \dfrac{1}{K_{f\,max}^A}$ — Effects of Notch Severity

$B = \dfrac{1}{1 + x\left(\dfrac{K_{f\,max}^B}{K_{f\,max}^A} - 1\right)}$ — Effects of Fabrication Distortion

$RS = 1 - \dfrac{\sigma_r}{\sigma_f'}$ — Effects of Residual Stresses

$MS = \dfrac{1}{\left(1+(2N_I)^b \dfrac{(1+R)}{(1-R)}\right)}$ — Effects of Applied Mean Stress

If the variables P, G, B, RS, and MS can be considered to be normally distributed variates, the COV of the fatigue strength of a weldment (Ω_S) can be approximated [2] as:

$$\Omega_S^2 \approx \Omega_P^2 + \Omega_G^2 + \Omega_B^2 + \Omega_{RS}^2 + \Omega_{MS}^2 + \Omega_f^2 \tag{4.4}$$

where:

Ω_P = COV of the random variable representing the effects of material properties.

Ω_G = COV of the random variable representing the stress-concentrating effects of geometry.

Ω_B = COV of the random variable representing the effects of welding-distortion-induced stresses.

Ω_{RS} = COV of the random variable representing the effects of notch-root residual stress.

Ω_{MS} = COV of the random variable representing the effects of applied mean stress.

The estimated sources of uncertainty in weldment fatigue strength data reported by various investigators [4] is tabulated in Table 4.2 together with the reliability factor (R_F, see Eq. 3.2). The squares of the COV of each of the factors P, G, B, RS, and MS are plotted in Fig. 4.13. As can be seen the sources of the scatter in weldment fatigue data depends upon the nature of the joint and how it is loaded. The butt joints (B1 and B2) have very little scatter associated with their reported fatigue data. The load carrying cruciform weldments (LCC1 and LCC2) have enormous scatter largely due to welding fabrication distortions which induce secondary stresses during gripping and subsequent axial loading. However, the estimated scatter in the fatigue data bank data is much

larger than that associated with even the "worst" weldment for the reasons discussed earlier in Chapter 3.

These observations are reflected in the plot (Fig. 4.14) of reliability factor (R_F). The values of R_f were obtained using Eq 3.2. The value of R_F for an individual weldment may be as high as 0.9 and as low as 0.7. Average values of $R_F$would seem to be around 0.7. The R_F implied by the use of a fatigue data bank entry for a particular weld geometry (e. g. Detail #10 in Fig. 4.1) is estimated at 0.55. The use of weld categories was earlier argued to lead to values of R_F of around 0.4.

The form of Eq. 4.4 suggests some interesting but perhaps obvious strategies for reducing the uncertainty in the fatigue strength of an individual weldment:

- If there is only one large source of uncertainty, the uncertainty in weldment fatigue strength can only be improved by its reduction; but the uncertainty in weldment fatigue strength can increase if any of the lesser sources is permitted to grow.
- If there is no dominant source of uncertainty, the uncertainty in weldment fatigue strength can only be improved by reducing all sources uniformly; but, as above, the uncertainty in weldment fatigue strength can increase if any one of the sources is permitted to grow.

4.11 Summary

In summary, weldment geometry, weld-distortion-induced bending stresses, and residual stresses are the main variables affecting the mean fatigue strength of a weldment. These variables are also the main contributors to the uncertainty in fatigue life. Analytical models can be used to estimate the uncertainty in fatigue strength and to identify the contribution of each source to the overall uncertainty.

TABLE 4.2 THE ESTIMATED SOURCES OF UNCERTAINTY IN WELDMENT FATIGUE STRENGTH DATA REPORTED BY VARIOUS INVESTIGATORS [4]

Data	Ω_P^2	Ω_G^2	Ω_B^2	Ω_{RS}^2	Ω_{MS}^2	Ω_S^{2*}	R_F
LCC1 - Load carrying cruciform (12.7 mm) [10,11]	.000946	.006410	.003870	0	.04507	.05630	.626
LCC2 - Load-carrying cruciform(6.35 mm) [10,11]	.000947	.010677	.004328	0	.02492	.02492	.731
NLCC1 - Non-load-carrying cruciform(32 mm) [9,12]	.001200	.003890	.006250	0	0	.01134	.808
NLCC2 - Non-load-carrying cruciform (25 mm) [13]	.000883	.005270	.000521	0	0	.01136	.808
B1 - Butt - Weldment(6 mm) [14,15,16]	.000814	.000661	.000811	.001394	0	.00365	.886
B2 - Butt Weldment(20 mm) [18,19,20]	.000862	.001280	.000941	.024916	0	.02800	.717
Data Bank - Butt Weldment: Single-V [17]	.004060	.009750	.081110	.001790	0	.09671	.545

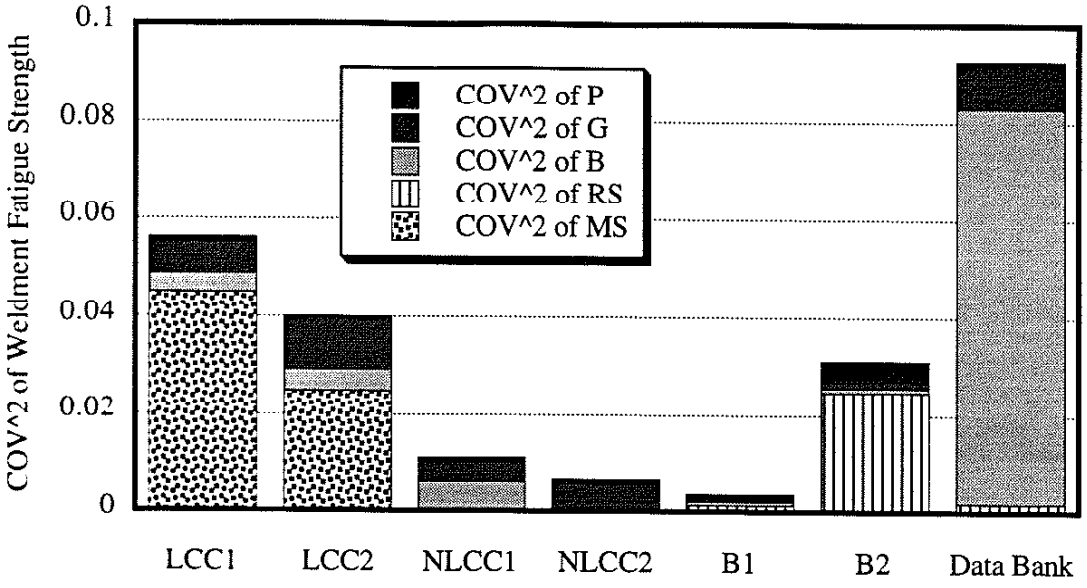

Fig. 4.13 Contribution of each of the factors P, G, B, RS, and MS to the COV^2 of the fatigue strength of the weldment at 10^6 cycles (Ω^2_Σ). The identity of the various weldments is given in Table 4.2

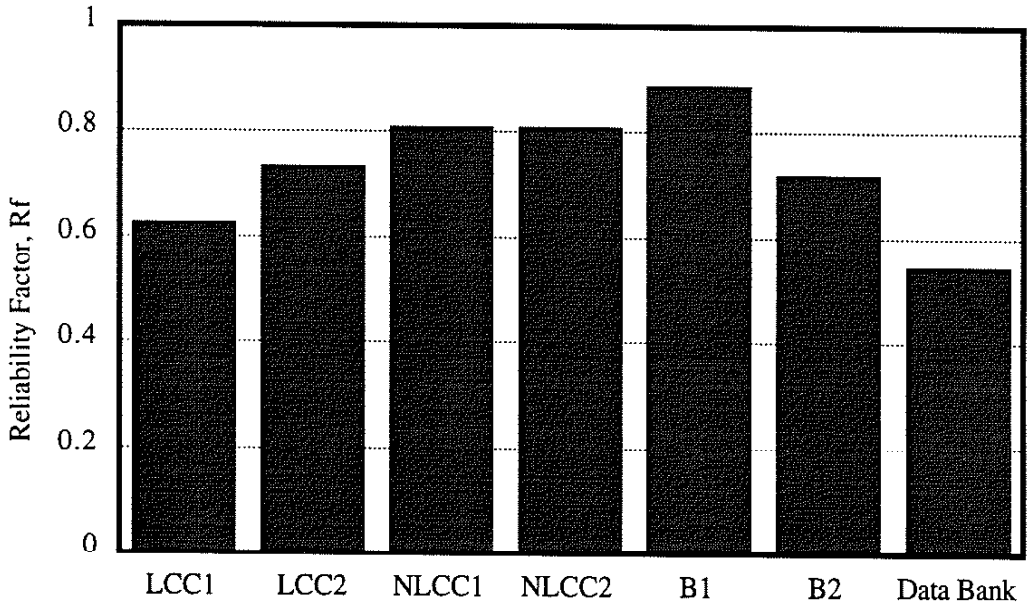

Fig. 4.14 The reliability factor (R_F) for each of the data sources in Table 4.2.

5.0 Conclusion

Organizing weldment fatigue behavior on the basis of fatigue crack initiation site reveals that the "Bad" joint geometries, weld terminations, are surprisingly severe. It is possible that weld discontinuities always play a large role in the fatigue behavior of weld terminations unlike the "Good" joint geometries which were considered in detail in this article. Unfortunately, the fatigue behavior of many joint geometries depends upon unknown or undefined quantities and is thus undefined. Despite their importance, these weldments were termed "Mavericks" and were not dealt with in this article.

The uncertainty in the fatigue life of a weldment, while not an attribute of the joint per se, is nonetheless as important as the mean strength in determining the design stresses in situations where great reliability is required. The uncertainty in the fatigue strength of weldments is perhaps not as large implied by the apparent scatter in either fatigue data for a given joint geometry or certainly by the scatter resulting from forcing many different joint geometries into a limited number of broad weld categories.

The variety of weldment joint geometries, materials, loading conditions, and post weld treatments will probably always force the engineer back into the testing laboratory, although in the future, computer simulations of weldment fatigue behavior will be able to answer many design questions. The computer simulations included in this work give guidance as to the exprected trends in weldment behavior, but these computer simulation results are offered with the understanding that they are to be intrepereted qualitatively.

Computer simulation results suggests that tensile welding residual stresses, tensile fabrication stresses, thick sections (large weldment size), and large preexisting discontinuities at the root of the critical notch all reduce the importance of fatigue crack initiation and early crack growth in weldments and thus reduce the fatigue strengths and fatigue lives of weldments. The most simple statement regarding the fatigue behavior of an individual weldment is that it depends upon whether or not fatigue crack initiation and early growth contribute substantially to its fatigue life. The large effect of weld quality and weldment size on weldment fatigue strength may explain the historic differences in the perceived behavior of weldments in light and heavy industries.

Computer simulation of weldment fatigue life suggests that the fatigue life and strength of "Ideal" weldments free of large discontinuities can be increased by post weld treatments which improve the weld geometry or alter the residual stresses, or both. In contrast, the computer simulation suggests that the fatigue life or strength of "Nominal" weldments containing large discontinuities can be most effectively improved by either eliminating the discontinuity or by controlling the fabrication residual stresses.

6.0 References

1. Munse, W. H., Wilbur, T. W., Tellalian, M. L., Nicoll, K. and Wilson K., "Fatigue Characterization of Fabricated Ship Details for Design," Ship Structure Committee, SSC-318, (1983).

2. Ang, A. H-S. and Munse, W.H., "Practical Reliability Basis for Structural Fatigue," Preprint No. 2459 for ASCE National Structural Engineering Convention at New Orleans, Louisiana during April 14-18, (1975).

3. Manual of Steel Construction, 8th Ed., American Institute of Steel Construction, Chicago, IL, 1980.

4. Park, S. K. and F. V. Lawrence, Jr., "Sources of Uncertainty in Weldment Fatigue Strength" Proceedings of the 9th International Conference of Offshore Mechanics and Arctic Engineering, ASME, Houston,1990, vol II pp 205 - 214.

5. Lawrence, F.V. and Dimitrakis, S.D., "I-P Model Simulation of the Factors Influening Weldment Fatigue Life," North American Welding Research Conference, EWI, 1995.

6. Maddox, S. J. and Andrews, R. M., "Stress Intensity Factors for Weld Toe Cracks," Proc. Conf. Computer aided assessment and controls of localized damage, Springer Verlag, Berlin, 1990.

7. Bell, R., and Vosikovsky, O. 1991. "Fatigue Life Prediction of Welded Joints for Offshore Structures under Variable Amplitude Loading," Offshore Mechanics and Arctic Engineering. Vol. III-B, Materials Engineering, 385 to 393.

8. Chang, S.-T. and Lawrence F.V., "Improvement of Weld Fatigue Resistance," FCP Report No. 46, College of Engineering, University of Illinois at Urbana-Champaign, (1986).

9. Engesvik, K. M. and Moan, T., "Probabilistic Analysis of The Uncertainty in the Fatigue Capacity of Welded Joints," Engineering Fracture Mechanics, Vol. 18, No. 4, pp 743-762, (1983).

10. Park, S.-K. and Lawrence F. V., "A Long-Life Regime Probability-Based Fatigue Design Method for Weldment," FCP Report No. 142, College of Engineering, University of Illinois at Urbana-Champaign, June (1988).

11. Park, S. K. and Lawrence, F. V., "Monte Carlo Simulation of Weldment Fatigue Strength", J. Construct,. Steel Research 12, (1989) pp. 279-299.

12. Engesvik, K. M., "Analysis of Uncertainties in the Fatigue Capacity of Welded Joints," Report No. UR-82-17, Department of Marine Technology, The University of Trondheim, Norway, (1982).

13. Lassen, T., and Eide, O. I., "Data for Fracture Mechanics Derivation of S-N Curves", The Ship Research Institute of Norway, (1984).

14. Nihei, M. Sasaki, E. Kanao, M, Inagaki, M., :Statistical Analysis of Fatigue Strength of Arc Welded Joints Using Covered Electrodes under Various Welding Conditions with Particular Attention to Toe Shape", Transactions of the National Research Institute for Metals, Vol. 23, No. 1, (1981).

15. Ohta, A., Kamakura, M., Nihei, Y., Inagaki, M., Sasaki, E., "An Automatic Detection of Fatigue Initiation Life of Welded Joints", Transactions of the National Research Institute for Metals, Vol. 22, No. 3, (1980).

16. Nihei, M., Yohda, M., Sasaki, E., "Fatigue Properties for Butt Welded Joints of SM50A High Tensile Strength Steel Plate", Transactions of the National Research Institute for Metals, Vol. 20, No. 4, (1978).

17. Radziminski, J. B., Srinivasan, J. B., Moore, R., Thrasher C., Munse, W. H., "Fatigue Data Bank and Data Analysis Investigation", Structural Research Series No. 405, Civil Engineering Studies, University of Illinois at Urbana-Champaign, (1973).

7.0 Acknowledgments

This article draws on the work of many people and many studies carried out over a period of years. The authors would like to acknowledge the advice and help of our colleagues at the UIUC in the Departments of Theoretical and Applied Mechanics and Mechanical Engineering. The article is based on several studies which were sponsored at various times by the UIUC Fracture Control Program, The Edison Welding Institute, the U. S. Coast Guard, and the Ship Structures Committee. The line drawings of Fig. 3.1 were drawn by Dr. Gregorz Banas.